

# Peer review status:

This document is a non-peer-reviewed preprint submitted to EarthArXiv.

The manuscript is currently under peer review at Remote Sensing of Environment.

The version posted here is the submitted (pre-review) version.

# Spatio-temporal Analysis of Vegetation Disturbance and Recovery in the Cerrado-Amazon Transition Using Landsat Time Series and Deep Learning

Chuanze Li<sup>a\*</sup>, Angela Harris<sup>a</sup>, Beatriz Schwantes Marimon<sup>b</sup>, Ben Hur Marimon Junior<sup>b</sup>, Matthew Dennis<sup>a</sup>, Ricardo Dalagnol<sup>c</sup> and Polyanna da Conceição Bispo<sup>a</sup>

#### Abstract

The Cerrado-Amazon Transition (CAT) represents the world's largest tropical ecotone, demarcating the boundary between the Brazilian Cerrado and Amazon biomes. Extensive deforestation and degradation within the CAT are driving irreversible ecological transformations and significant biodiversity loss. The escalating incidence of fire and agriculture-induced deforestation has rendered the CAT a dynamic ecological frontier, situated within the globally recognized 'Arc of Deforestation'. However, our understanding of deforestation and ecosystem degradation in the CAT is limited due to insufficient knowledge regarding the spatial and temporal patterns of these disturbances. Here, we utilize satellite image time-series segmentation combined with a convolution neural network (CNN) to identify and quantify disturbances within the CAT over a 35-year period. Using the Landtrendr algorithm, Landsat time-series data, and a Residual Neural Network (ResNet), we categorized four distinct types of disturbances—Amazon forest clear-cutting, Cerrado clear-cutting, Amazon forest fire, and Cerrado fire-based on their temporal-spectral trajectories and disturbance-recovery patterns. We identified over 384,000 km<sup>2</sup> of land cover disturbance between 1986 and 2020, with Amazon forest clear-cutting accounting for the largest proportion (35%) of the detected changes. In the southern CAT, disturbances in the Cerrado vegetation were widespread, while in the northern CAT, Amazon forest disturbances indicated a gradual loss of native forest boundaries. Our findings also reveal that whilst fire caused less immediate damage to vegetation than clear-cutting, neither the Amazon forest nor the Cerrado vegetation fully recovered to their pre-fire conditions within a decade post fire. These findings emphasize the necessity of adopting targeted conservation strategies and restoration measures to mitigate the long-term ecosystem degradation of this critical ecological transition zone.

Keywords: Cerrado - Amazon Transition (CAT); Landsat time series; LandTrendr; Residual Neural Network; Vegetation disturbance; Cleat-cutting and fire; Vegetation recovery

### 1. Introduction

The Cerrado-Amazon Transition (CAT) zone is the Earth's largest tropical ecotone, serving as a critical boundary between Brazil's Cerrado savanna and the Amazon rainforest Biomes (Marques et al., 2020). Spanning 6,000 km, the CAT hosts a highly diverse array of plant species and structural formations (Marques et al., 2020; Projeto RADAMBRASIL, 1981), as it encompasses transitional vegetation types from both the Amazon rainforest and the Cerrado savanna. This ecological diversity contributes to its dynamic boundaries and results in substantial spatial heterogeneity in vegetation cover, biomass, and carbon storage capacity (de Souza Mendes et al., 2019; Marques et al., 2020; Ratter et al., 1973; Torello-Raventos et al., 2013). Yet, despite its ecological significance, the CAT endures a multitude of environmental pressures from both anthropogenic and natural sources, particularly deforestation and fire.

Driven largely by the Large-scale expansion of agriculture and pasturelands, clear-cutting has become

<sup>&</sup>lt;sup>a</sup>Department of Geography, School of Environment, Education and Development, University of Manchester, Oxford Road, Manchester M13 9PL, UK

<sup>&</sup>lt;sup>b</sup>Universidade do Estado de Mato Grosso, Campus de Nova Xavantina, Nova Xavantina, MT, 78690-000, Brazil <sup>c</sup>CTREES, Pasadena, 91105 California, USA

<sup>\*</sup>Correspondence: chuanze.li@postgrad.manchester.ac.uk

the dominant disturbance in the CAT (Flores et al., 2024; Ribeiro et al., 2024), causing cascading ecological consequences such as vegetation carbon loss (Coe et al., 2013; Maia et al., 2010), biodiversity decline (Almeida et al., 2018; Wearn et al., 2012), and soil degradation (Bonini et al., 2018; Hunke et al., 2015). Fire activity has also been widespread across the CAT over the past four decades (Ribeiro et al., 2024), primarily caused by human activities, including the use of fire for land clearing and management (Cerri et al., 2018; Matricardi et al., 2013), and the conversion of land for agriculture and cattle ranching, which increases the accumulation of flammable biomass (Fearnside, 2005). Whilst previous studies have documented patterns of fire occurrence and clear-cutting in specific sites or sub-regions near the Amazon–Cerrado boundary (Marques et al., 2024; Reygadas et al., 2021; Souza et al., 2021), there remains limited understanding of where, when and how frequently disturbances occur across the broader CAT region. This knowledge gap is primarily a consequence of the CAT's ecological and spatial complexity, which poses significant challenges for disturbance detection and identification.

Understanding how vegetation recovers after disturbance is essential for assessing ecosystem resilience, estimating carbon fluxes, and guiding long-term land management and conservation strategies. Incomplete or slow recovery can lead to sustained carbon emissions, shifts in biome boundaries, and feedbacks that disrupt regional hydrology and global climate systems (Aragão et al., 2018; Pellegrini et al., 2018; Silva Junior et al., 2020). In the CAT zone, only a limited number of studies have examined vegetation responses to disturbance using field-based approaches (e.g., Reis et al., 2017, 2015), often relying on data from relatively small 100 m<sup>2</sup> plots. These provide valuable insights into localized recovery processes but lack the spatial coverage to inform regional-scale patterns. Complementary remote sensing efforts, such as Santana et al., (2020), have assessed post-fire vegetation trends using 250 m MODIS data over 15 years in parts of the CAT, offering a broader but coarser perspective. While these studies have advanced our understanding, it remains uncertain whether their findings are representative of the broader and ecologically diverse CAT ecotone. Some research suggests that seasonally dry forests in the CAT may be more fire-resilient due to lower fuel loads and fire-adapted species (Balch et al., 2011; Hoffmann et al., 2012; Ribeiro and Walter, 2008), whereas seasonally flooded Amazonian forests become highly fire-sensitive during droughts as their moisture-rich root systems dry out and become flammable (Maracahipes et al., 2014). However, the extent to which these contrasting recovery patterns apply across the CAT remains poorly understood.

Moreover, while numerous studies have explored post-disturbance recovery within the Amazon or Cerrado biomes individually (e.g., Bullock and Woodcock, 2021; Drüke et al., 2023; Machida et al., 2021; Silva et al., 2018), extrapolating their findings to the CAT is problematic due to its ecological complexity and transitional nature. A critical knowledge gap remains: we lack a comprehensive understanding of how different vegetation types within the CAT respond to various disturbance regimes over time and space. Addressing this gap requires the integration of long-term satellite time series with advanced classification and modeling approaches to capture and compare recovery trajectories across the full extent of the ecotone.

EO data are often used for large-scale temporal vegetation monitoring (Wang et al., 2019). A variety of time-series detection algorithms—such as LandTrendr (Kennedy et al., 2010), VCT (Huang et al., 2009), CCDC (Zhu and Woodcock, 2014), and BFAST (Verbesselt et al., 2010) — have been developed to analyze EO image stacks and identify both abrupt and gradual changes in vegetation (Fang et al., 2018; Ma et al., 2020; Novo-Fernández et al., 2018; Zhou et al., 2024). Among these, LandTrendr was specifically designed for Landsat time series and has been effectively utilized to detect both abrupt disturbance events and recovery patterns within forests across America, Amazonia, China, and Cerrado biome (Almeida de Souza et al., 2020; Kennedy et al., 2010; Reygadas et al., 2021; Yin et al., 2022). Temporal-spectral trajectory features, which can be obtained from time-series detection algorithms, have also been used to identify specific types of disturbance events, particularly when integrated with traditional machine learning models (Hermosilla et al., 2015; Li et al., 2022; Murillo-Sandoval et al., 2018; Zhao et al., 2015). For example, Murillo-Sandoval et al., (2018) applied BFAST and Random Forest to differentiate conversion to pasture, conversion to agriculture, and non-stand replacing disturbance in Amazon biome; and (Zhao et al., 2015) combined VCT with Support Vector Machine to

separate wildfires, harvests, and other disturbance categories in Greater Yellowstone Ecosystem. However, the use of EO data for improving our understanding of disturbance dynamics with the CAT is limited. Those that have used EO data, have primarily focused on static land cover mapping or have identified change within the CAT by comparing maps of vegetation cover over a limited number of points in time (de Souza Mendes et al., 2019; Morton et al., 2006; Wang et al., 2019; Zaiatz et al., 2018). While these thematic maps are useful for tracking major shifts in land use, they often fail to detect lower-intensity disturbances, and they fail to capture the temporal dynamics of vegetation responses, which limits our understanding of post-disturbance recovery processes in this ecologically heterogeneous region.

In this study we use a new methodological approach to produce the first detailed characterization of the temporal and spatial patterns of major disturbances (i.e. fire and clear-cutting of vegetation) within the CAT. We use a novel two-step framework utilising Landsat time series data: first the LandTrendr algorithm is used to identify vegetation disturbances; and second a deep learning model (ResNet) is used to classify disturbance categories based on the full temporal trajectory of affected pixels. To our knowledge, this is the first attempt to integrate time-series disturbance detection with deep learning-based attribution in a complex tropical ecosystem such as the CAT. In contrast to conventional machine learning approaches, which typically rely on handcrafted temporal metrics derived from time series (Hermosilla et al., 2015; Li et al., 2022; Murillo-Sandoval et al., 2018; Zhao et al., 2015), deep learningbased method directly utilizes the full temporal trajectory, enabling the extraction of high-level features and contextual patterns across time, improving classification accuracy =(Chen et al., 2021). Moreover, this modular approach, by decoupling the detection of change from land cover classification, not only alleviates the need for large-scale, fully annotated training datasets, but also lowers the overall computational burden by limiting classification tasks to pre-identified regions of interest (Pfeiffer et al., 2023). This framework enables a shift from simple land cover change detection to a more process-based understanding of disturbance and recovery, ultimately providing a more nuanced characterization of vegetation dynamics in tropical ecotones. Specifically, we focus on identifying dynamic changes that have over a 35-year period (1986-2020). Through our analysis we aim to identify the locations and timings of the most severe disturbance events, and to determine how the rate of vegetation recovery varies, both between key vegetation types found within the CAT, and in response to different disturbance drivers. We expect that expanding anthropogenic disturbances are gradually eroding the Amazon forest frontier, and hypothesise that fire-affected Amazon forest vegetation will demonstrate rapid but often incomplete recovery, whilst the more fire-adapted Cerrado vegetation will recover more rapidly and completely. These hypotheses guide our analysis and form a basis for interpreting vegetation recovery patterns in this ecologically critical transition zone.

#### 2. Material and Methods

# 2.1. Study area

The study area encompasses a total of 1,145,247 km², stretching from the southwest to the northeast along the transitional belt between the Cerrado and Amazon biomes (IBGE, 2019; Fig. 1). Given the absence of an officially recognized boundary for the CAT, the extent of the study area was defined to encompass locations of existing vegetation survey plots (i.e. Plant Ecology Laboratory of the Universidade do Estado do Mato Grosso) that have been widely used to understand vegetation dynamics with the CAT region (Faria et al., 2024; Lenza et al., 2015; Marimon et al., 2014; Marques et al., 2020; Reis et al., 2015). The region's climate is primarily classified as Tropical Savanna with a dry winter (Aw) and Tropical Monsoon (Am) according to the Köppen classification system. The average annual temperature ranges from 24.1°C to 27.3°C, with localized dry-season temperatures reaching up to 45°C (Araújo et al., 2021; Reis et al., 2018).

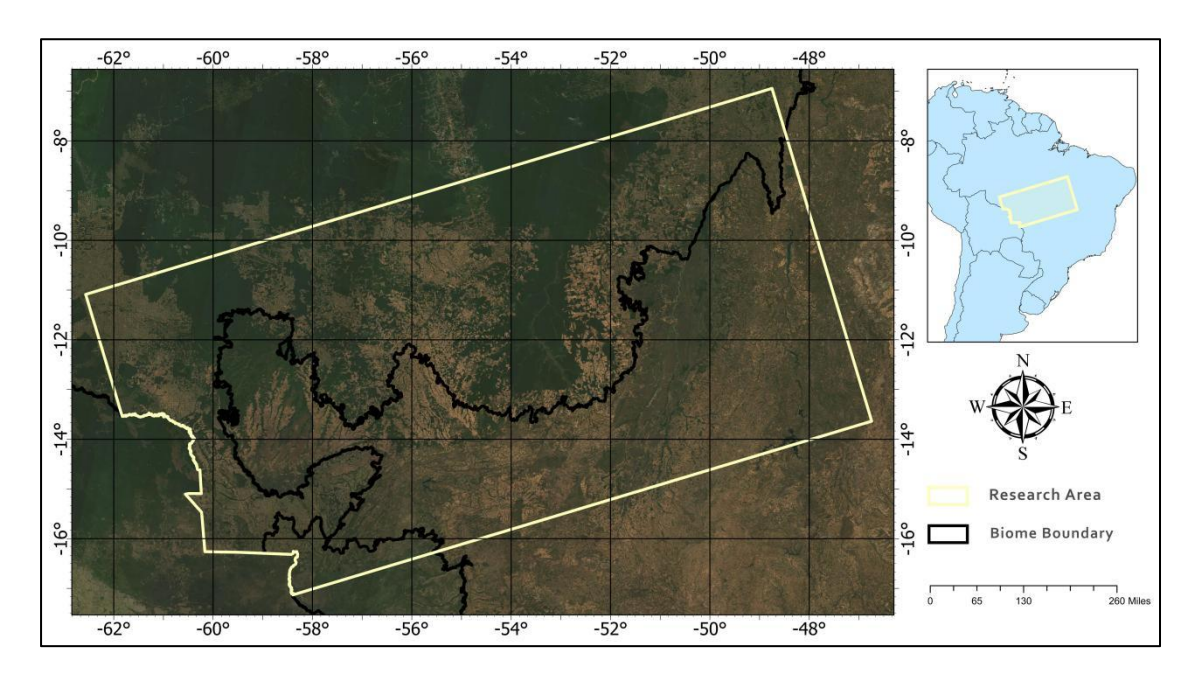


**Fig. 1.** The location of the CAT, encompassing part of the Brazilian States of Mato Grosso, Pará, Tocantins and Goiás. The yellow border depicts the research area; the black border is the traditional dividing line of biomes in Brazil with the Amazon biome to the north, the Cerrado biome to the south and the Pantanal at the southwest corner, near Cuiabá (IBGE, 2019). The background image is a composite of cloud-free Landsat 8 OLI scenes acquired between Jan 1 and Dec 30, 2021.

Based on the ecological heterogeneity found within the CAT, we grouped the vegetation types used in this study into two major categories; namely Amazon forest and Cerrado, with each encompassing several structurally distinct vegetation subtypes (Table 1).

Table 1. Classification and structural characteristics of Amazon forest and Cerrado within the CAT.

| Categories | Description   | References   |
|------------|---|--|
| Amazon     | Includes open ombrophilous forests, seasonal forests, gallery forests, and dry forests, primarily distributed north of the traditional biome boundary. These  | (Marimon et al., 2014, 2006;   |
| Forest     | forests are generally more continuous and closed-canopy, with taller trees and higher biomass than Cerrado.  Mainly located south of the traditional biome boundary, the Cerrado comprises  | Ratter et al., 1973)   |
| Cerrado    | a gradient of vegetation types:  — Cerradão (woodland savanna): Trees 8–15 m tall, canopy cover 50%–90%, featuring a mix of Amazon and Cerrado species, typically in contact zones between dry forests and other Cerrado vegetation.  — Dense Cerrado: Trees 5–8 m tall, canopy cover 50%–70%  — Typical Cerrado: Trees 3–6 m tall, canopy cover 20%–50%  — Open Cerrado: Trees 2–3 m tall, canopy cover 5%–20% | Gonçalves et al., 2021; Marimon et al., 2014; Marimon Junior and Haridasan, 2005; Marques et al., 2020; Oliveira et al., 2017; Ratter et al., 1973 |

#### 2.2. Methods

Fig. 2 presents an overview of the methodological approach employed to identify and understand the dynamics of disturbances in the CAT from 1986 to 2020. Initially, we identified the presence of disturbance events using Landsat annual medoid composite images and the LandTrendr disturbance detection algorithm (Kennedy et al., 2010) within Google Earth Engine (Fig.2a; GEE: Gorelick et al., 2017). Subsequently, for each identified disturbance event, we extracted temporal trajectories of individual Landsat spectral bands (NIR, SWIR1, SWIR2) and calculated spectral indices (NBR, NDMI, TCB, TCG, TCW, TCA; Table 2). The temporal trajectory data were then used as input variables for a deep-learning model (ResNet), to classify each of the disturbance events into four categories: (i) Amazon forest clear-cutting, (ii) Amazon forest fire, (iii) Cerrado clear-cutting, and (iv) Cerrado fire (Fig.2b) indicating both the predominant type of vegetation present and the type of disturbance that had occured. Finally, we constructed disturbance-recovery trajectories based on values of the normalized burn ratio (NBR) for each identified disturbance category, and quantified differences in post-disturbance responses across these four disturbance categories using two spectrally-derived indicators: the Relative Differenced Normalized Burn Ratio (RdNBR; Miller et al., 2009) and the Recovery Indicator (RI; Kennedy et al., 2012; Fig. 2c).

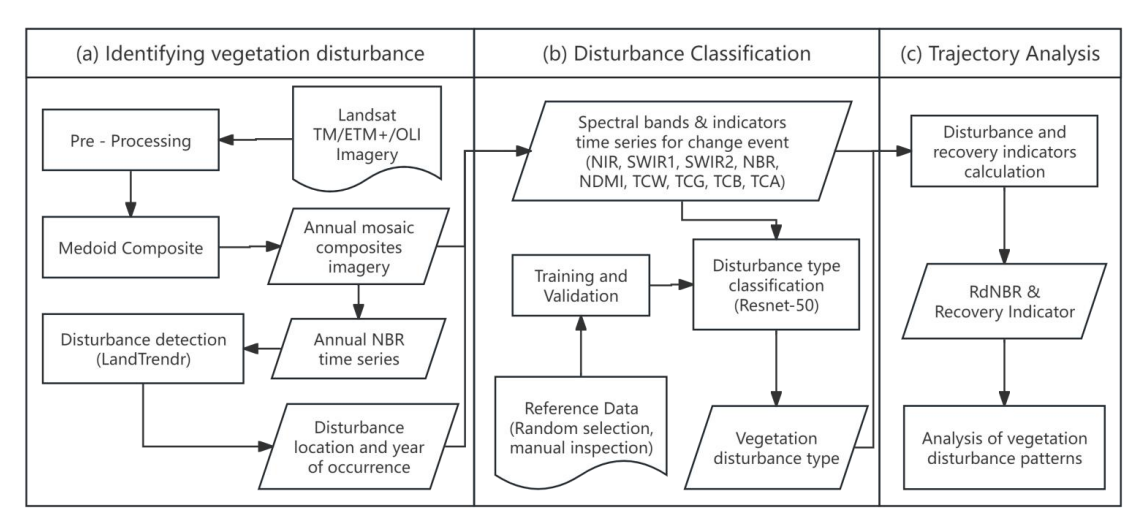


Fig. 2. Overall research approach. Abbreviations and their meaning are described in Table 4.

#### 2.2.1. Data description

We acquired Landsat Tier 1 surface reflectance data for the CAT region for each dry season (June 1 to September 30) from 1985 to 2020. The data were harmonized across multiple Landsat sensors, including Landsat 5 Thematic Mapper (TM), Landsat 7 Enhanced Thematic Mapper Plus (ETM+), and Landsat 8 Operational Land Imager (OLI), using the equations provided by Roy et al., (2016). Clouds and cloud shadows were masked using FMASK-derived quality assurance bands(Zhu and Woodcock, 2012), and annual composites were generated using the medoid compositing method. Although our primary focus is on the period beginning in 1986, we included data from 1985 as the LandTrendr algorithm used for detecting breakpoints in the time series requires at least one year of pre-disturbance imagery (Kennedy et al., 2018).

We used the MapBiomas History of deforestation (MapBiomas, Collection 8), the MapBiomas History of Fire Scars (MapBiomas, Collection 3), and the Deforestation and Degradation in Tropical Moist Amazon forest (TMF) data from the European Commission's Joint Research Centre data products (Vancutsem et al., 2021) as reference data to aid in the preliminary selection of areas for the generation of the disturbance classification training dataset. The key characteristics of these datasets are summarized in Table 2.

# **Table 2.** Key characteristics of reference datasets.

| Dataset                                   | Description  | Method  | Spatial Scope                    | Source  |
|---|--|---|----------------------------------|---|
| MapBiomas<br>History of<br>Deforestation  | Estimates forest and non-forest vegetation loss across biomes based on pixel-wise land cover change.   | Track year-to-year changes in land<br>cover and land use by comparing<br>Annual land cover/use maps<br>(Collection 8)                       | Brazil-wide                      | https://brasil.mapbiomas.org/en/metodo-desmatamento/  |
| MapBiomas<br>History of Fire<br>Scars     | Detects fire scars using<br>burned/unburned samples and deep<br>learning. But it does not distinguish<br>between the types of vegetation<br>where fires occur. | Deep Neural Network on Landsat<br>imagery samples, with reference to<br>MODIS burned areas product<br>(MCD64A1) and burn scars from<br>INPE | Brazil-wide                      | https://brasil.mapbiomas.org/en/metodo-mapbiomas-fogo |
| TMF (Tropical<br>Moist Forest)<br>Dataset | Tracks deforestation and degradation trajectories over 34 years using Landsat time series. But it does not include savanna regions like the Cerrado biome.     | Spectral-temporal trajectory analysis from Landsat (1990–2024)  | Global tropical<br>humid forests | https://forobs.jrc.ec.europa.eu/TMF/data#factsheets   |

# 2.2.2. Identifying vegetation disturbance

We applied the LandTrendr time segmentation and fitting algorithm within GEE to detect vegetation disturbances within the CAT based on time series trajectories of the Normalized Burn Ratio (NBR: Key and Benson, 2006). The LandTrendr algorithm operates on the principle that the temporal evolution of a pixel can be approximated by a series of linear segments. Stable periods are represented by segments with minimal slope, whereas disturbances are indicated by segments with abrupt changes in value, followed by recovery segments exhibiting a gradual increase, potentially returning to the original pixel value. The algorithm's output is a fitted spectral trajectory represented by multiple interconnected segments for each pixel within the study area (Fig. 3; Kennedy et al., 2010).

The selection of appropriate model parameters for the LandTrendr algorithm is crucial for accurate processing(Kennedy et al., 2018). To detect multiple change events without overfitting the model, the Maximum Number of Segments was set to nine based on trial and error. The spike threshold was set to 0.75 to reduce the overestimation of disturbance magnitude caused by sudden breakpoints. Additionally, to exclude the effects of NBR fluctuations within the normal range expected for vegetation (especially in the Cerrado biome) and to eliminate bare ground, only disturbance events with pre-disturbance NBR values greater than 0.2 and a modeled magnitude greater than 0.15 were considered.

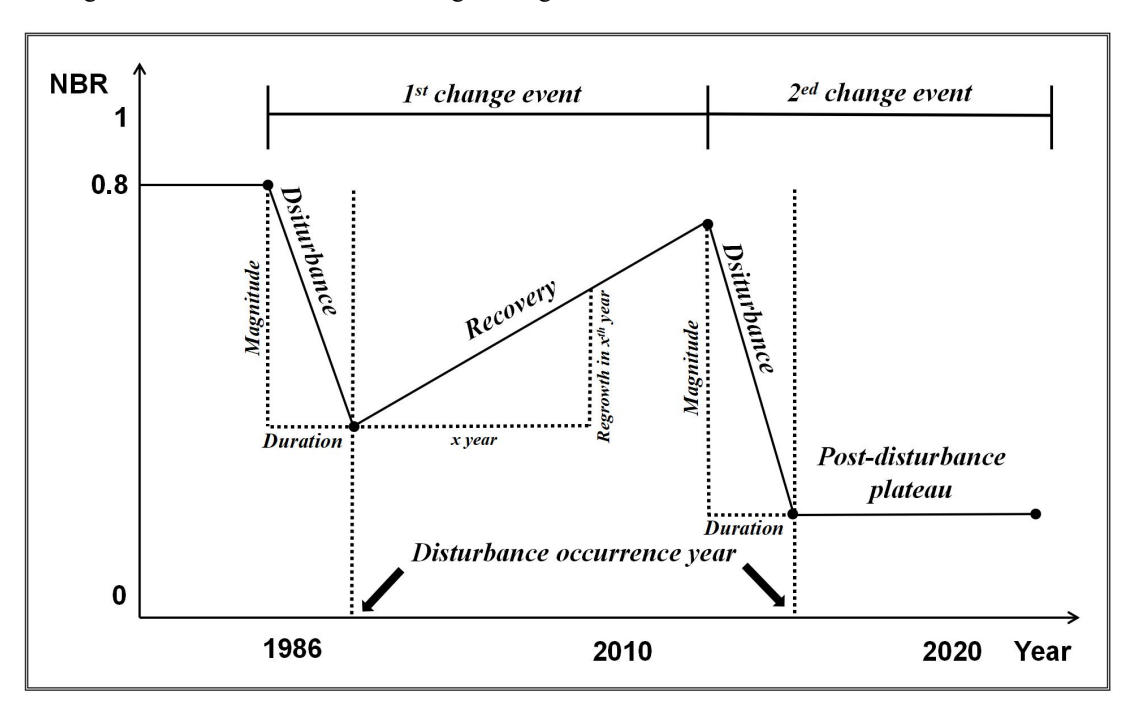


Fig. 3. Conceptual example of the disturbance and post disturbance Normalized Burn Ratio (NBR) fitted trajectory. Concept example showing two change events at the same location, with quantitative indicators of disturbance and recovery.

We define a change event as consisting of two components: (i) the disturbance, characterized by a decreasing trend in a time-series segment, and (ii) the post-disturbance, which consists of one of two predefined temporal trajectories namely a) recovery, characterized by a positive trend in the time-series segment following a disturbance event, continuing until a subsequent disturbance event is detected within the same pixel or b) a post-disturbance plateau, characterized by a stable NBR value maintained and showing no evidence of recovery within the time series (Fig. 3). The post-disturbance plateau may occur

when forest loss is driven by agricultural or pasture expansion, indicating prolonged suppression of natural vegetation regeneration due to continuous human activity.

To avoid detecting gradual long-term disturbances, such as those resulting from slow vegetation degradation, we identified only those change events where disturbances lasted less than two years and the recovery or post-disturbance plateau time exceeded one year. Where multiple disturbance events occurred in the same location but in different years, we repeated the analysis outlined above to obtain information for each disturbance event. Our analysis focuses on a maximum of three disturbance events for each pixel as more than three disturbance events were rarely observed. As our study focused on disturbances to natural vegetation, as opposed to disturbances caused by clear-cutting of secondary forests or pasture fires, prior to analysis we masked all areas of non-natural vegetation that were present before 1985 using land use and land cover type data from Mapbiomas. In the subsequent disturbance classification process (see section 2.2.3), we also excluded all disturbance events detected after a clear-cutting event was identified as the land cover post disturbance is likely to be different to that which was originally disturbed (e.g. clear-cutting of a forest for agricultural purposes is unlikely to result in the subsequent re-growth of a similar forest in the same location). Fire disturbances do not necessarily result in land use type conversions (Andela et al., 2017); therefore, secondary disturbances occurring after fire events were retained for analysis.

We evaluated the accuracy of vegetation disturbance detection results using TimeSync (Cohen et al., 2010), which is an interpretation tool for change detection algorithm calibration and map validation based on Landsat trajectories and Google Earth high-resolution imagery. The validation dataset consisted of 542 pixels, the size of which was determined according to the formula of Cochran, (1977):

$$n = \frac{z^2 p(1-p)}{d^2} \tag{1}$$

where z = 1.96 (representing a 95% confidence interval), d is the half-width of the confidence interval, and p is the expected overall accuracy of the population under simple random sampling. We set 0.94 as the value of p, based on 94% estimation accuracy (Reygadas et al., 2021), and set d as 0.02.

According to the area ratio of disturbed and non-disturbed areas, we randomly sampled and verified 249 disturbed pixels and 293 non-disturbed pixels across the study area. For each selected validation pixel, we conducted a visual inspection of the NBR trajectory and the associated time series of Landsat images to ascertain (i) whether a disturbance event had occurred and, if so (ii) the specific year in which the disturbance occurred.

# 2.2.3. Classification of Disturbance Events

We aimed to classify four types of vegetation disturbance events based on the temporal trajectories of disturbance pixels identified by the LandTrendr algorithm (Table 3). To construct robust training and validation datasets for this classification task we first used the MapBiomas deforestation and fire products, as well as the TMF deforestation dataset (Section 2.2.1), to identify areas with a high likelihood of disturbance. This spatial filtering step reduced the search space and improved the efficiency of sample selection. Within these candidate areas, we randomly selected sample points that had also been independently detected as disturbances by the LandTrendr algorithm (Section 2.2.2), thereby ensuring consistency with our time series-based disturbance framework. For each selected sample point we used the TimeSync tool to manually verify and classify both the vegetation type and the specific disturbance category based on Landsat time series and high-resolution imagery. To mitigate potential sampling bias and ensure an even spatial distribution, we applied a minimum distance constraint of 300 meters between selected points. Ultimately, we obtained a balanced dataset by selecting 2,000 pixels for each of the four

disturbance categories. Ultimately, These labeled samples were randomly split into training (80%) and validation (20%) datasets for model development and evaluation.

Table 3. Classification and description of vegetation disturbance events.

| Event Type                  | Description   |
|-----------------------------|---|
| Amozon forest alone sytting | The complete removal of forest cover in the Amazon biome, typically through land clearing,    |
| Amazon forest clear-cutting | leaving the land devoid of trees.   |
| Cerrado clear-cutting       | The full removal of natural vegetation in the Cerrado biome, including both woody and grassy  |
| Cerrado ciear-cutting       | vegetation, usually for agricultural or land development purposes.                            |
| Amazon forest fire          | The damage or degradation of Amazon forests caused by uncontrolled or deliberate fires, which |
| Amazon forest me            | may not result in complete deforestation but can lead to significant ecological disturbances. |
| Cerrado fire                | The disruption of the natural balance in the Cerrado biome due to fire, which can alter       |
| Cerrado fire                | vegetation composition and ecosystem function, but may not entirely eliminate plant cover.    |

We used the one-dimensional residual network (ResNet; He et al., 2016), to classify the disturbance category based on the temporal trajectories of disturbance pixels identified using the LandTrendr algorithm. The 1D-CNN architecture is primarily employed to extract information from linearly structured time series datasets and has been extensively used in vegetation and crop monitoring and classification (Bai et al., 2023; Li et al., 2021; Ma et al., 2023). Specifically, we used the ResNet-50 model (Koonce, 2021) implemented in the Python TensorFlow library. The model was trained using a batch size of 64, where each sample corresponds to a 90-length time-series vector representing a single pixel. We used a learning rate of  $\eta = 0.001$  and optimized the model with the Adaptive Moment Estimation (Adam) algorithm for mini-batch gradient descent. For each training pixel the temporal trajectories of three spectral bands and six spectral indices (Table 4) were used as inputs to the classifier, as previous studies have shown that including multiple spectral indices can reduce noise and improve classification accuracy (Shimizu et al., 2019). For pixels identified by the LandTrendr algorithm as having experienced a single disturbance within the study period, the time series trajectory began the year before the date that the disturbance was detected and continued for 10 years afterward. The 10-year time frame was selected based on the results of Chen et al., (2021), which demonstrated that a 10-year time frame has a lower error rate than other time-series lengths in monitoring and classifying deforestation and fire events by CNN (convolution neural network). In cases where multiple disturbances were detected, separate time series trajectories were extracted for each event. To handle cases where the time-series trajectory was shorter than 10 years, such as disturbances occurring after 2012 or in pixels that experienced subsequent disturbances within a 10-year window, the final year of the trajectory was replicated to ensure a uniform time-series length across all samples. The ResNet model primarily captures local features via convolutional layers and is less sensitive to the sequence order (Wei-Jian et al., 2021), thus we concatenated the nine time series trajectories for each pixel (corresponding to three bands and six indices) into a single sequence of length of 90 to simplify its structure for improved computational efficiency. All time-series samples were normalized to the range -1 to 1 in order to accelerate model convergence and stabilize training (Salimans and Kingma, 2016). We also compared the classification output from Resnet-50 with a random forest model (ntrees = 200, mtry = 9) through the use of a confusion matrix and user accuracy, producer accuracy, and overall accuracy statistics were obtained and compared for both outcomes.

**Table 4.** Spectral bands and vegetation indicators used for vegetation disturbance monitoring and classification, Blue, Green, Red are the visible blue, visible green and visible red bands, respectively.

| Name                                       | Abbreviation | Formula/Band Range  | Features   | Reference  |
|--|--------------|---|--|--|
| Near-Infrared<br>Reflectance               | NIR          | 0.75 - 1.4 μm   | Sensitive to chlorophyll content of living vegetation.   | 4 1D E   |
| Shortwave<br>Infrared 1                    | SWIR1        | 1.55 - 1.75 μm  | Sensitive to water content in soil and vegetation, lignin content of non-  | Avery and Berlin,<br>1992; Miller and<br>Thode, 2007                                     |
| Shortwave<br>Infrared 2                    | SWIR2        | 2.08 - 2.35 μm  | photosynthetic vegetation, and hydrous minerals.   | Thoue, 2007  |
| Normalized<br>Burn Ratio                   | NBR          | $NBR = \frac{NIR - SWIR2}{NIR + SWIR2}$   | Not easily saturated and sensitive to viable chlorophyll, leaves, soil moisture content, char and ash. Responses to different types of disturbance (e.g., vegetation clearcutting, fire, pests and diseases, etc.) are evident.  Highly correlated with canopy water | Bright et al.,<br>2019; Key, 2006;<br>Key and Benson,<br>2006; Schroeder et<br>al., 2011 |
| Normalized<br>Difference<br>Moisture Index | NDMI         | $NDMI = \frac{NIR - SWIR1}{NIR + SWIR1}$  | content, it can track changes in plant<br>biomass and water stress and therefore<br>respond more effectively to less severe<br>disturbance events.   | DeVries et al.,<br>2015; Gao, 1996;<br>Ochtyra, 2020                                     |
| Tasseled Cap<br>Brightness                 | ICB          | [TCB] [0.2043 0.4158 0.5524 0.5741 0.3124 0.2303] [Blue Green]  | TCB provides an indication of the overall pixel reflectance, TCG provides an   | Banskota et al.,   |
| Tasseled Cap<br>Greenness                  | ICG          | $ TCG  = \begin{vmatrix} -0.1603 - 0.2819 - 0.4934 \ 0.7940 - 0.0002 - 0.1446 \ NIR \end{vmatrix}$  | indication of vegetation photosynthetic conditions, and TCW is highly sensitive to   | 2014; Crist and<br>Cicone, 2007;   |
| Tasseled Cap<br>Wetness                    | TCW          | SWIR1   SWIR2   SWIR2 | changes in Amazon forest structure.  | Healey et al., 2006  |
| Tasseled Cap<br>Angle                      | TCA          | $TCA=arctan\left(\frac{TCG}{TCB}\right)$  | TCA reveals the ratio of vegetation to non-<br>vegetation, with TCA in harvested areas<br>being significantly lower than in any other<br>Amazon forest cover stage.  | Gómez et al.,<br>2011; Schroeder et<br>al., 2011   |

# 2.2.4. Disturbance and recovery trajectory analysis

We generated quantitative trajectory indicators from the model-fitted NBR time series to understand how vegetation within the CAT responded to different types of disturbance events. For each disturbance event that we identified (sections 2.2.2 and 2.2.3), we calculated two key indicator trajectories. The first index quantified the level of vegetation damage caused by the disturbance, as it uses pre and post disturbance values of NBR to calculate the RdNBR, which determines the relative change in vegetation post disturbance (equation 2).

$$RdNBR = \frac{\Delta NBR}{\sqrt{ABS(NBR_{predis})}} \tag{2}$$

Where  $\triangle NBR$  is the NBR change in disturbance,  $NBR_{predis}$  is the absolute value (non negative) of NBR before disturbance.

We also calculated the RI, which quantifies the degree of vegetation recovery following a disturbance event The RI is the ratio of post-disturbance regrowth to the level of vegetation lost during the preceding disturbance event (Equation 3). Since clear-cutting typically signifies a land-use conversion, which precludes vegetation recovery, the RI metric was only calculated for fire events. We standardized the assessment of post-disturbance recovery to a 10-year period as preliminary analysis of the data indicated little year-to-year variation in NBR for recovery periods longer than 10 years. If the recovery period was shorter than 10 years, the RI was calculated up to the final year of the available recovery trajectory.

$$RI = \frac{NBR_{y+x} - NBR_{y}}{\Delta NBR}$$
 (3)

Where  $NBR_y$  is the NBR value in the disturbance year y, and  $NBR_{y+x}$  is the NBR value in the  $x^{th}$  year after the disturbance. We used analysis of variance (ANOVA) to determine whether the degree of disturbance (i.e. RdNBR) and recovery (i.e RI) differed between four different disturbance categories.

#### 3. Results

# 3.1. Reliability and Regional Variation of Disturbance Detection

Despite the diverse vegetation types present in the CAT zone, the LandTrendr algorithm achieved an overall disturbance detection accuracy of 80% (Table 5). Whilst some disturbed pixels were not identified (~24 %) by the LandTrendr algorithm, 80% of the pixels that were identified as disturbed were correct as compared with the reference data. These results suggest that while our estimates of disturbance within the CAT region may be underestimated, we have a high degree of confidence that the pixels identified as disturbed accurately represent true disturbances.

Table 5. Confusion matrix and performance assessment of disturbance identification in the CAT region.

|                    |                     | LandTrendr<br>Test Data |             |           |                 |  |
|--------------------|---------------------|-------------------------|-------------|-----------|-----------------|--|
|                    |                     | Disturbed               | Undisturbed | Row Total | User's accuracy |  |
| Classified<br>Data | Disturbed           | 189                     | 48          | 237       | 80%             |  |
|                    | Undisturbed         | 60                      | 245         | 305       | 80%             |  |
|                    | Total               | 249                     | 293         | 542       |                 |  |
| ひ                  | Producer's accuracy | 76%                     | 84%         |           |                 |  |
|                    | Overall accuracy    |                         |             | 80%       |                 |  |

Over the 35-year period, 33% of the study area (384,717 km²) experienced at least one disturbance event. Fig. 4 presents the spatial patterns of disturbance events and the years in which each disturbance was detected. The most recent disturbance events (orange to yellow in colour) were found to the far North of the CAT dividing line towards the natural vegetation of the Amazon biome, and also tend to be spatially clustered (Fig. 4a). In contrast, disturbances in the region south of the CAT boundary in the Cerrado biome were more temporally heterogeneous and their spatial distribution was more dispersed (Fig. 4b).

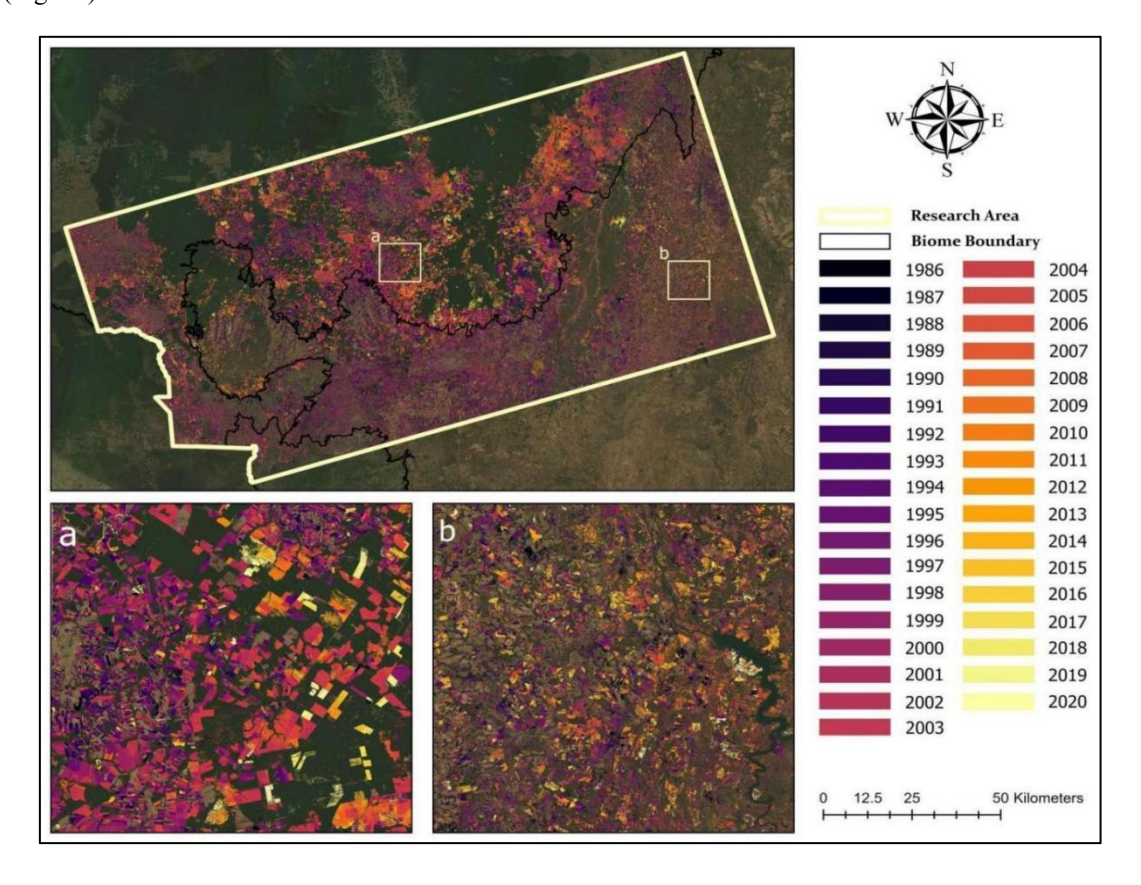


**Fig. 4.** Spatial distribution of first vegetation disturbance occurrence time detected in CAT between 1986 and 2020. Illustrations of regional spatial details showing (a) Amazon forest disturbance erode natural vegetation boundaries over time chosen for its representativeness of widespread deforestation trends; (b) heterogeneous pattern of Cerrado disturbance events, chosen because of its representation of the diverse landscape characteristics of the Cerrado biome. The background image is a composite of cloud-free Landsat 8 OLI scenes acquired between Jan 1 and Dec 30, 202.

# 3.2. Identifying different types of vegetation disturbance

Our findings indicate that disturbance categories can be accurately mapped using temporal disturbance trajectories in conjunction with the ResNet classification architecture, achieving an overall classification

accuracy of 95%, which outperformed the random forest model in terms of both producer and user accuracy (Table 6). Fig. 5 provides examples of the temporal trajectories that are characteristic of different mapped disturbance categories. Amazon forest clear-cutting and fires resulted in more pronounced changes in spectral and vegetation indicators compared to disturbance observed in the Cerrado vegetation. Clear-cutting in both the Amazon forest and Cerrado vegetation resulted in more abrupt and longer-lasting change in spectral and vegetation indicators compared to fire disturbances. Among all indicators, NBR and NDMI exhibited the most pronounced changes in magnitude between pre- and post-disturbance conditions, regardless of the disturbance category.

Table 6. Classification Accuracy of disturbance category in the CAT region.

|   | ResNet-50<br>True labels |                |               |         |          |  |  |
|---|--------------------------|----------------|---------------|---------|----------|--|--|
|   | Amazon forest            | Cerrado clear- | Amazon forest | Cerrado | User's   |  |  |
|   | clear-cutting            | cutting        | fire          | Fire    | accuracy |  |  |
| Amazon forest clear-cutting   | 399                      | 11             | 3             | 8       | 95%      |  |  |
| Cerrado clear-cutting   | 3                        | 381            | 0             | 10      | 97%      |  |  |
| Amazon forest fire  | 5                        | 0              | 383           | 7       | 97%      |  |  |
| Cerrado Fire  | 3                        | 18             | 4             | 365     | 94%      |  |  |
| Producer's accuracy   | 97%                      | 93%            | 98%           | 94%     |          |  |  |
| Total accuracy  | 95%                      |                |               |         |          |  |  |
|   | Random Forest            |                |               |         |          |  |  |
| Producer's accuracy Total accuracy  Amazon forest clear-cutting Cerrado clear-cutting | 354                      | 14             | 14            | 3       | 92%      |  |  |
| Cerrado clear-cutting   | 35                       | 360            | 0             | 20      | 87%      |  |  |
| Amazon forest fire  | 11                       | 3              | 367           | 2       | 96%      |  |  |
| Cerrado Fire  | 10                       | 33             | 99            | 365     | 88%      |  |  |
| Producer's accuracy   | 86%                      | 88%            | 94%           | 94%     |          |  |  |
| Total accuracy  |                          |                | 90%           |         |          |  |  |

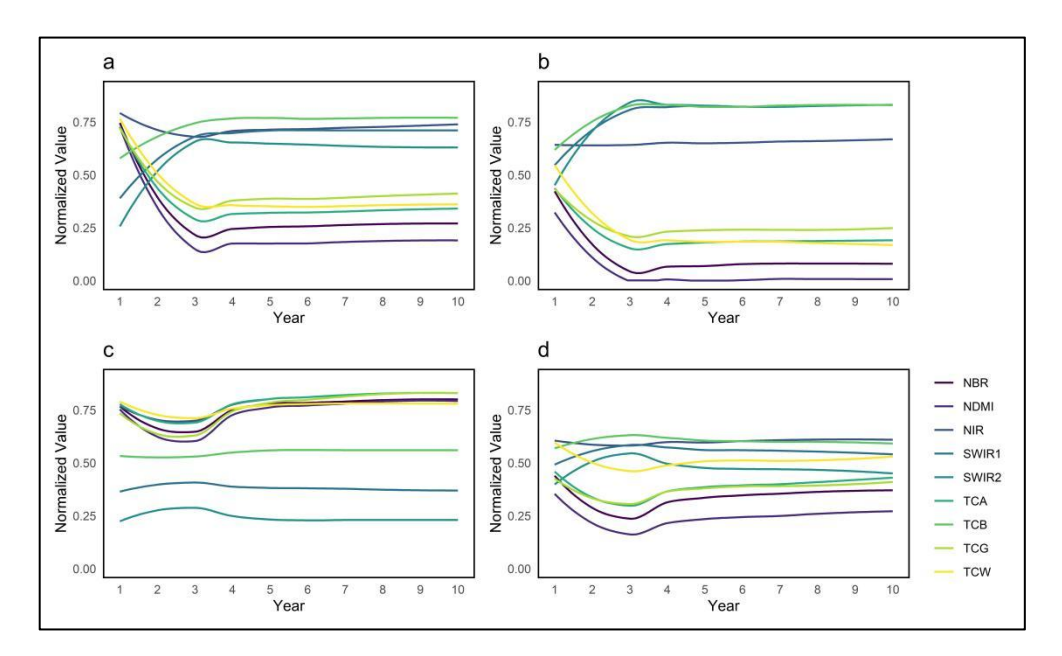
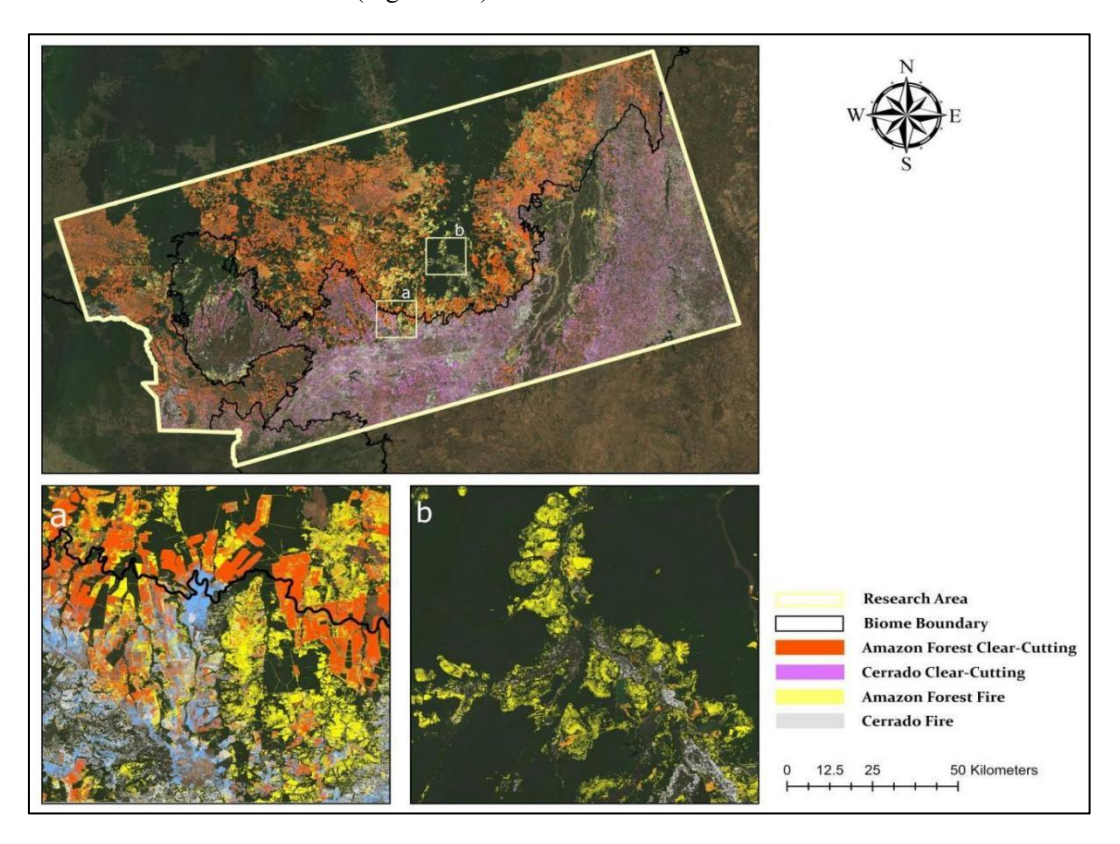


Fig. 5. Mean values of the time series of spectra and vegetation indicators for different vegetation disturbance categories in the disturbance classification model. (a) Amazon forest clear-cutting; (b) Cerrado clear-cutting; (c) Amazon forest fire; (d) Cerrado fire. Abbreviations are defined in Table 4.

Our disturbance classification results show that Amazon forest clear-cutting was the main type of disturbance in the CAT zone between 1985 - 2020 and accounted for 35% (167,347 km²) of the total disturbed area. Forest clear-cutting was widespread across the CAT and frequently found north of the traditional ecological boundary (Fig. 6&7a). In contrast to wide-spread forest clear-cutting, forest disturbances caused by fire tended to be more spatially clustered, smaller in size, and often located adjacent to forested areas that had been clear-cut (Fig. 6a). Forest fires were also often observed along river corridors (Fig 6b).

Unlike Amazon forest disturbances, our results showed that disturbances that occured in Cerrado vegetation were primarily in the southern part of the CAT. Cerrado disturbances were often smaller than those occurring in Amazon forest vegetation and were distributed across the landscape in a scattered and irregular manner (Fig. 6a). However, similar to Amazon forest vegetation, a clear spatial association was observed between disturbed Cerrado vegetation affected by clear-cutting and fire, indicating spatial co-occurrence of these disturbances (Fig. 7 b&d).



**Fig. 6.** Spatial distribution of first vegetation disturbance categories detected in CAT between 1986 and 2020 and examples of regional spatial details showing (a) fires occurring around clear-cutting areas and (b) fires occurring along rivers.

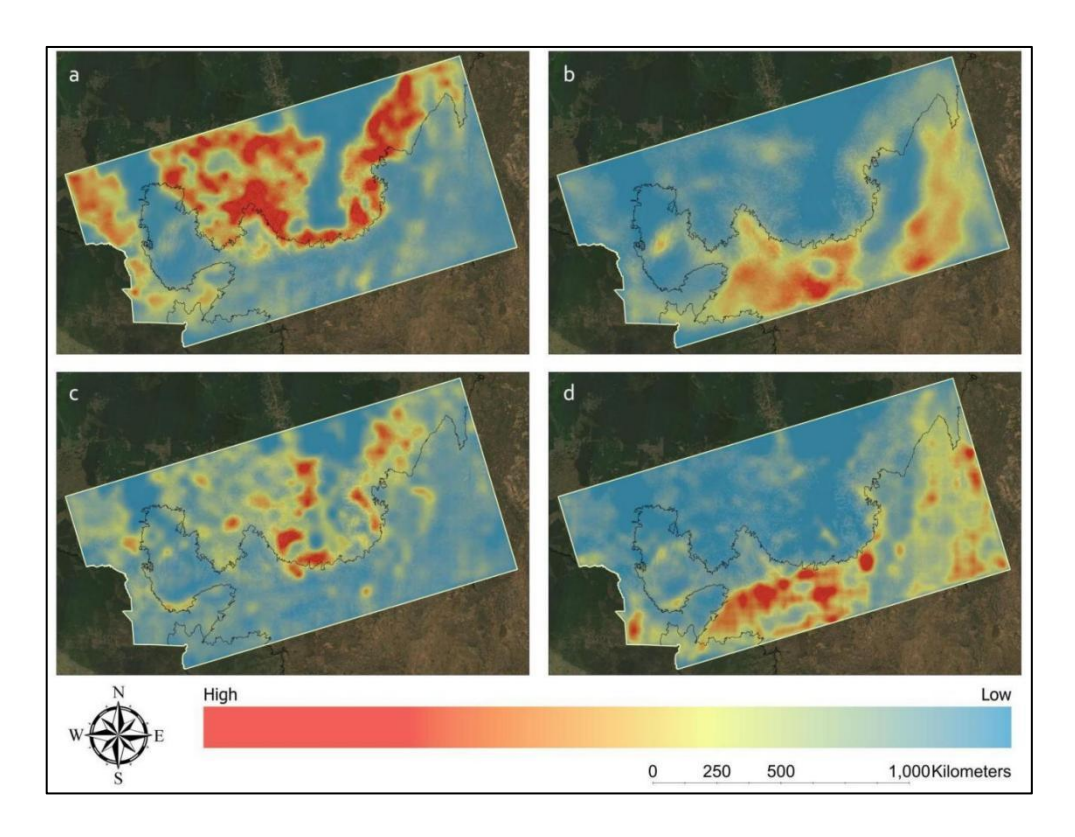


Fig. 7. Distribution of high frequency areas by disturbance category. (a) Amazon forest clear-cutting, (b) Cerrado clear-cutting, (c) Amazon forest fire, (d) Cerrado fire in the CAT. The maps were generated by interpolating the cumulative disturbance area within each 1000×1000-pixel grid cell (900 km²). If multiple disturbances occurred at the same pixel during the study period, each event was included in the total area calculation.

Fig. 8 illustrates the temporal dynamics of the Amazon forest and Cerrado disturbances between 1986 and 2020. Our results show a positive trend in the total disturbed area prior to 1998 followed by another increase in the area affected by clear-cutting in the Amazon forest vegetation between 2002 and 2004 (Fig. 8a). Our analysis also indicates that in the Amazon forest vegetation, an increase in the area disturbed by fire following increases in the area disturbed by clear-cutting, suggesting a potential lagged relationship (Fig. 8a); whereas in the Cerrado vegetation, the area affected by both types of disturbances show a synchronous temporal pattern (Fig. 8b).

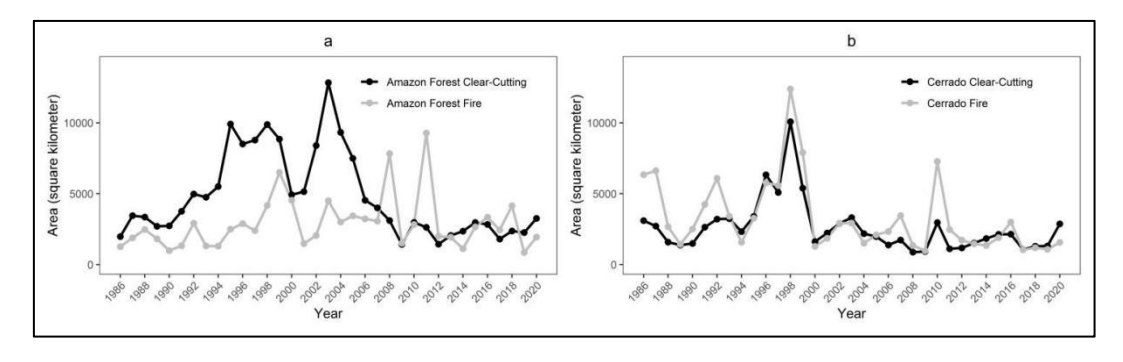
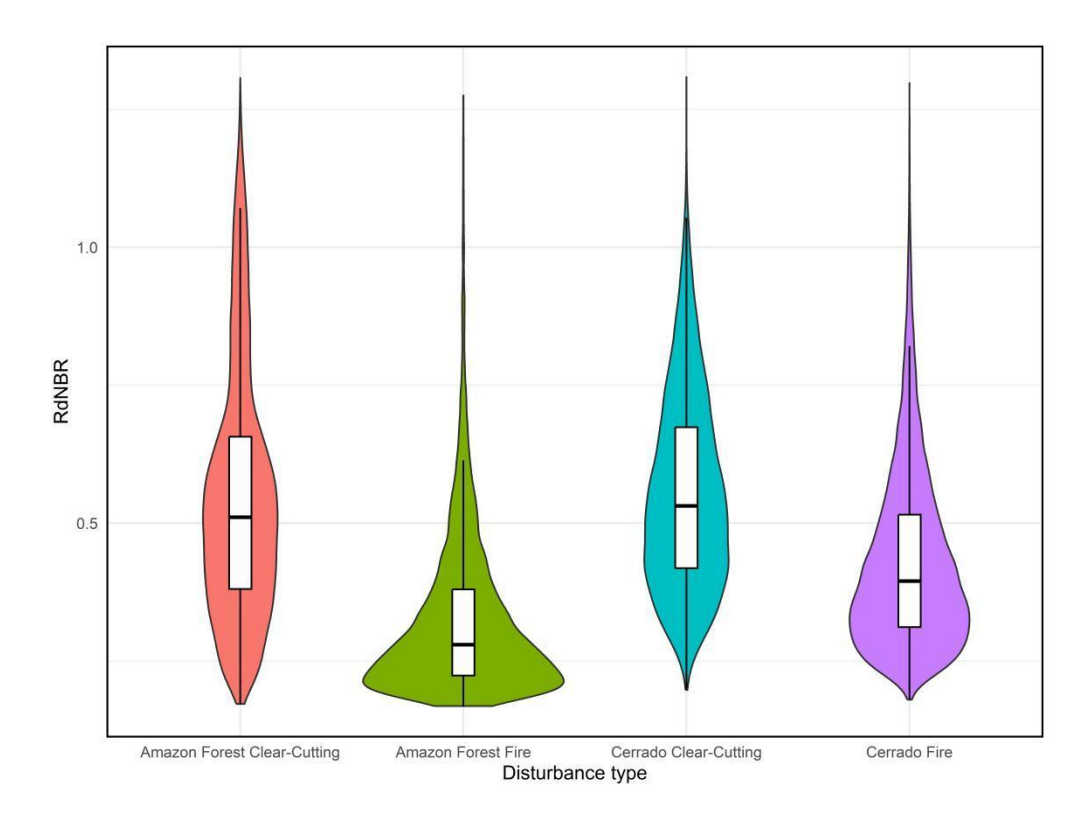


Fig. 8. Temporal dynamics of vegetation disturbance in the (a) Amazon forest vegetation and (b) Cerrado vegetation.

# 3.3. Influence of the type of disturbance on vegetation disturbance-recovery trajectories

We calculated the RdNBR to quantify and compare the level of vegetation damage due to different types of disturbance events. Our results indicate that the vegetation damage of the disturbance endured differs according to the type of disturbance event (Table 7; F=3959, p<0.001). As expected, we found that on average, fire disturbances were associated with lower vegetation damage—as indicated by lower RdNBR values—compared to clear-cutting, in both Cerrado vegetation and Amazon forest vegetation within the CAT (Fig. 9). Our results also suggest that many of the fire disturbances identified within the Amazon forest vegetation were of low damage, compared to those observed in the Cerrado vegetation, whereas clear-cutting had a very similar impact on both types of vegetation communities (Fig. 9).



**Fig. 9.** A violin plot of the distribution of RdNBR values for the different disturbance categories identified from the ResNet deep learning classification in the CAT, based on 50,000 randomly sampled pixels.

**Table 7.** Comparisons between RdNBR values for the different types of disturbance events identified in the CAT based on a random sample of 50,000 pixels.

| Comparison            |                             | Mean difference | Std. Error | t value (Tukey) | p value (Tukey) |
|-----------------------|-----------------------------|-----------------|------------|-----------------|-----------------|
| Amazon forest fire    | Amazon forest clear-cutting | -0.226          | 0.002      | -96.290         | < 0.001         |
| Cerrado Clear-Cutting | Amazon Forest Clear-Cutting | 0.009           | 0.002      | 3.943           | < 0.001         |
| Cerrado Fire          | Amazon Forest Clear-Cutting | -0.115          | 0.002      | -52.676         | < 0.001         |
| Cerrado Clear-Cutting | Amazon Forest Fire          | 0.231           | 0.003      | 88.007          | < 0.001         |
| Cerrado Fire          | Amazon Forest Fire          | 0.106           | 0.002      | 42.605          | < 0.001         |
| Cerrado Fire          | Cerrado Clear-Cutting       | -0.125          | 0.003      | -49.339         | < 0.001         |

We also compared the recovery of vegetation cover in Amazon forest and Cerrado vegetation following fire disturbance, as indicated by changes in the annual RI. Our findings revealed that vegetation began to regrow quickly within both the Amazon forest and Cerrado vegetation, recovering to approx 80% of pre-fire levels in the Amazon forest vegetation by the end of the time series, but only 60% of the pre-fire levels in the Cerrado vegetation (Fig. 11). Notably, neither vegetation type fully returned to pre-disturbance conditions within a ten-year period, as indicated by an annual RI value <1.

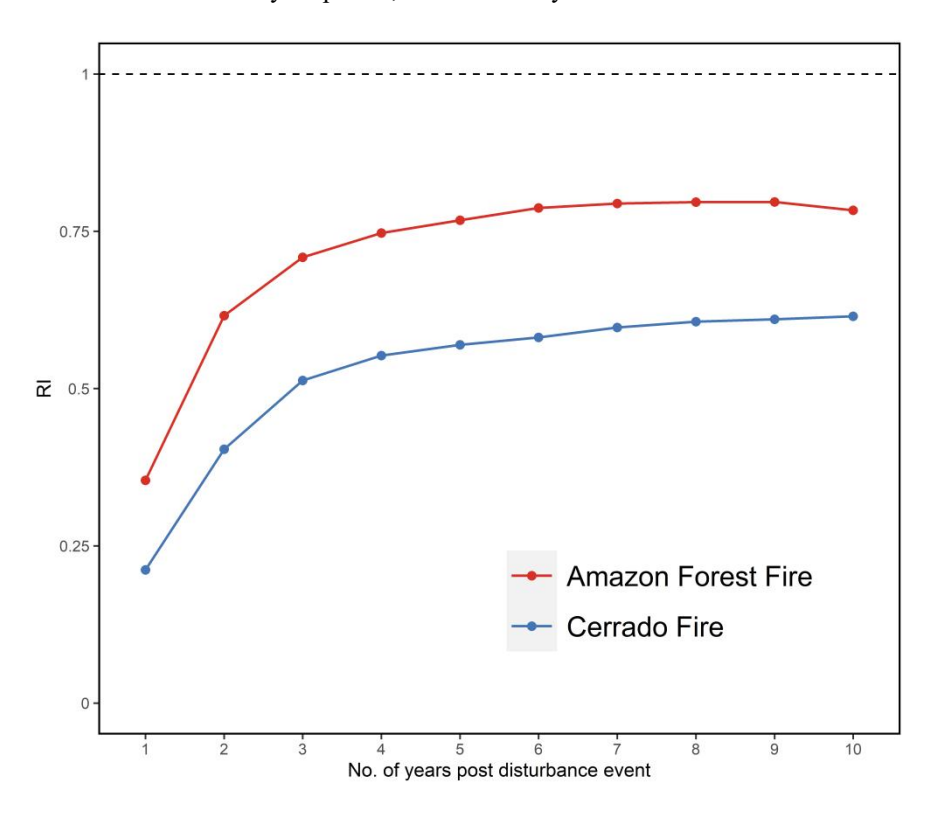


**Fig. 10.** Annual Recovery Indicator (RI) of different disturbance categories present within the CAT. An RI value of 1 indicated that vegetation cover has returned to pre-disturbance levels. The plots have been generated from 50,0000 randomly sampled pixels.

### 4. Discussion

The CAT represents an ecotonal region of exceptional ecological significance, where the Amazon forest and Cerrado vegetation converge to create a heterogeneous landscape that supports high biodiversity (Maracahipes-Santos et al., 2015; Marques et al., 2020). Using the novel combination of time-series analysis of EO data together with a deep-learning model, our study provides a unique insight into the extent and intricate spatial patterns of vegetation disturbances within the ecologically sensitive CAT region over the last 35 years.

With the increasing length of EO data records, time-series-based vegetation monitoring techniques offer expanded opportunities for studying disturbances. We show that the LandTrendr algorithm in combination with the ResNet-50 model can be used to detect and classify vegetation disturbances in complex spatially heterogeneous ecosystems with a high level of overall accuracy (80% & 95%; Table 5 & 6). While variations in parameters and threshold selection inherent to the LandTrendr algorithm may complicate consistent application across different vegetation types, the overall accuracy remains high. The ResNet-50 classifier significantly outperformer than the more traditional random forest approach (Table 6), which showed lower accuracy for clear-cutting than fire events - likely because clear-cutting is

typically followed by diverse land use practices (e.g., agriculture, pasture), resulting in greater spectral variability. Compared to previous studies that applied deep learning techniques in less complex environments, our approach maintains or exceeds similar levels of classification accuracy. For example, Maretto et al., (2020), Dalagnol et al., (2023) and Mota et al., (2024) reported accuracies between 76%-95% in relatively homogeneous Amazon biome using deep learning, While studies in savanna-forest mosaics have often faced challenges due to overlapping structural and phenological characteristics (Bendini et al., 2022). Achieving similar or higher accuracies in a spatially and temporally dynamic ecotone such as the CAT indicates that our approach is not only robust but particularly suited for heterogeneous environments. The reason for this robustness lies in the ability of Deep learning techniques to extract long-term spectral patterns and complex disturbance signals by integrating complex non-linear signals in time (Perbet et al., 2024). Furthermore, our workflow requires relatively limited training data compared to typical deep learning applications, as the disturbance trajectories were pre-structured by the LandTrendr segmentation. This two-step framework reduces the data burden and enhances the model's scalability to larger regions and multi-year applications—an important consideration for operational EObased disturbance monitoring in data-scarce regions. In summary, our study provides empirical evidence that integrating temporal segmentation algorithms with residual convolutional architectures offer a robust and scalable solution for detecting and characterizing multi-type vegetation disturbances, especially within ecologically heterogeneous and temporally dynamic tropical landscapes.

Using Landsat time series and the LandTrendr algorithm combined with a ResNet-50 model, our results suggest that Amazon forest clear-cutting has been the cause of the most widespread disturbances within the CAT over the last 35 years, accounting for approximately 35% of the total disturbed area (Fig. 6). The Amazon forest clear-cutting gradually erodes the edges of intact vegetation (Fig. 4a). Driven largely by agricultural expansion, Amazon forest vegetation continued to be the primary target for conversion into croplands and pastures (Fig. 6). Similar patterns of persistent and large-scale clear-cutting have previously been observed along the so-called "Arc of Deforestation" and are often associated with the progressive incursion of agricultural zones into forested landscapes (Arvor et al., 2017; Matricardi et al., 2020; Ribeiro et al., 2025; Verburg et al., 2014). Our results suggest that in the CAT, Amazon forest clear-cutting reached a peak around the year 1998 (Fig. 8a), and the underlying temporal dynamics reflect the influence of economic shifts, policy changes, and market conditions. For example, the broader liberalization of Brazil's economy in the early 1990s and the introduction of the Real Plan in 1994which stabilized inflation and attracted agribusiness investment—are often cited as factors that contributed to agricultural expansion across the Amazon and Cerrado biomes (Myers, 2023). Global commodity demand and rising crop prices during the late 1990s may have further accelerated land clearing during this period (Harding et al., 2021; Nepstad et al., 2006; Ouma, 2020). Following this peak, a decline in clear-cutting is observed after 2000 (Fig. 8a), which related to the Plano Real having sharply cut the rate of inflation. By the end of 1997, land prices reportedly dropped by around 50%, reducing the appeal of land speculation (Fearnside, 2005). Our results also indicate that a second wave of Amazon forest clear-cutting emerged in 2004 (Fig. 8a), which coincides with evidence of a global surge in commodity demand and agricultural prices, which also lead to increased agricultural production in the CAT (Bacha and Vinicios de Carvalho, 2014; Harding et al., 2021; Nepstad et al., 2006; Ouma, 2020). Another possible contributing factor is the weakening of environmental oversight and enforcement capacity in the CAT region, which occurred around 2002 due to a significant reduction in IBAMA's field personnel and limited resources, leaving large areas without effective monitoring or control (Barreto, 2006). Notably, to this day, while protected areas currently cover approximately 28% of the Amazon biome, only 2% of this protection falls within the boundaries of our study area (According to conservation data from Mapbiomas), highlighting the CAT's institutional vulnerability (Carneiro et al., 2024; Pokorny et al., 2021, 2013; Pokorny and Pacheco, 2014; Ros-Tonen et al., 2008).

In contrast to the concentrated disturbance patterns observed in Amazon forest vegetation, our results show that disturbances to Cerrado vegetation were spatially dispersed (Fig. 4b), which is consistent with the decentralized pattern of land conversion typically observed in the wider Cerrado biome (Rosan et al., 2022; Sawyer, 2008). Unlike the Amazon forest vegetation, where large contiguous tracts of forest are

often targeted for conversion, land-use change in the Cerrado vegetation tends to occur in smaller, scattered patches due to both the mosaic nature of the Cerrado vegetation landscape (Martello et al., 2023) and the decentralized expansion of agricultural frontiers (Sano, 2019). This pattern contributes to a subtler but persistent erosion of ecological integrity over time (Dionizio and Costa, 2019; Gomes et al., 2019; Lucas et al., 2023). A key factor shaping this process is the Cerrado biome's limited legal protection relative to the Amazon biome. While nearly 80% of the Amazon biome is covered by legal environmental frameworks, only 35% of the Cerrado biome within the "Legal Amazon" and 20% outside it fall under similar protection(Carneiro et al., 2024; Colman et al., 2024; De Marco Jr et al., 2023; Luiz and Steinke, 2022). The discrepancies in governance have resulted in uneven enforcement and monitoring efforts, allowing for continued expansion of agricultural activities in more vulnerable Cerrado biome. Our results show that by 1998 large-scale Cerrado clear-cutting had substantially reduced vegetation cover (Fig. 8; Marques et al., 2024; Vieira et al., 2022), leading to a subsequent decline in clearing activities in subsequent years.

Our results also identified a strong temporal and spatial association between clear-cutting and fire in both the Amazon forest and the Cerrado vegetation found within the CAT (Figs. 7 & 8), likely driven by the intentional use of fire to expand grazing land (Andreoni and Londoño, 2019; Medeiros and Fiedler, 2011; Pivello et al., 2021) and to prepare soils for agriculture (Arroyo-Kalin, 2012; Gomes et al., 2019). For example, our results showed that fire disturbances were frequently located near pastures (Fig. 4c), while Amazon forest fires were also commonly observed along riverbanks (Fig. 4b). These riparian zones often overlap with indigenous territories (Golin, 2024), where traditional slash-and-burn practices continue (Ferreira de Alencar Mendes et al., 2023; Schmidt et al., 2021). Notably, Amazon forest fire activity often peaked several years after clear-cutting, whereas Cerrado fire and clear-cutting tended to occur simultaneously. This divergence reflects different land management practices: in the Amazon, fire is commonly used as a post-clearing tool to manage regrowth and prepare land for pasture, while in the Cerrado, fire is more frequently employed as a direct clearing method and to condition soils for cropping (Arroyo-Kalin, 2012; Gomes et al., 2019).

Understanding how different vegetation types respond to disturbance is critical for evaluating ecosystem resilience and informing effective conservation and land management strategies. In this study, we employed trajectory-based indicators to quantify both the severity of vegetation damage and the rate of post-disturbance recovery across the Amazon forest and Cerrado within the CAT region, focusing specifically on disturbances caused by clear-cutting and fire. Our results reveal that fire events in the CAT tend to cause greater and more prolonged damage to Cerrado vegetation compared to adjacent forested areas (Fig. 9). To our knowledge, this is the first regional-scale, Earth observation-based study to compare fire impacts across these two contrasting vegetation types within the CAT. Although Cerrado ecosystems are often described as fire-adapted, previous studies indicate that their structural characteristics—such as open canopies and a grass-dominated understory—make them highly flammable (Durigan and Ratter, 2016; Miranda et al., 2009; Rodrigues et al., 2021). During the dry season, rapid desiccation and the build-up of fine fuels significantly increase fire intensity, frequently resulting in widespread topkill of woody vegetation (Hoffmann et al., 2012).

This vulnerability is further amplified by human-induced ignitions, which have become increasingly frequent and severe in recent years (Alvarado et al., 2017; da Silva Arruda et al., 2024; Melo et al., 2021). Our findings provide empirical, landscape-scale evidence that supports these concerns and highlights the susceptibility of Cerrado vegetation to fire-driven degradation, even in regions where fire has historically been part of the disturbance regime. In contrast, the Amazon forest's closed canopy appears to buffer fire effects by preserving soil moisture and limiting the accumulation and exposure of fine fuels (Connell and Slatyer, 1977; Dormann et al., 2020). However, fire-induced losses beneath dense forest canopies may be underestimated by satellite sensors due to limited spectral penetration, suggesting that some impacts on forest structure and regeneration dynamics may remain undetected.

While both Amazon forest and Cerrado vegetation began to show signs of post-fire recovery within approximately three years, our results indicate that both vegetation types failed to return to pre-fire levels, even a decade post-fire (Fig 10) (Silva et al., 2018; Souza-Alonso et al., 2022). This aligns with our initial

expectation regarding the Amazon forest vegetation, whose recovery is often incomplete (Silva et al., 2018; Souza-Alonso et al., 2022) due to the compounding effects of extreme climate events, such as increasingly frequent droughts (Alencar et al., 2011; De Faria et al., 2021a, 2021b), and anthropogenic fire recurrence that limits the forest's ability to regenerate fully between events (De Faria et al., 2021a, 2021b). However, contrary to our expectations, despite being a fire-adapted ecosystem the Cerrado vegetation did not recover more rapidly or more completely than the Amazon forest. This finding challenges the conventional understanding that the Cerrado vegegtation generally recovers more rapidly after fire (Hoffmann, 2005; Moreira, 2000), which may reflect recent changes in disturbance regimes. Repeated anthropogenic fires have disrupted the Cerrado vegetation's natural fire-adapted equilibrium, pushing the ecosystem beyond its recovery thresholds (Alvarado et al., 2017; Hoffmann et al., 2012). The cumulative impacts of such fires reduce structural integrity, limit regeneration potential, and ultimately undermine long-term ecological resilience (Attri et al., 2020; Pinty et al., 2000; Souza-Alonso et al., 2022). It is important to note that recovery detected by satellite imagery is mainly related to increases in canopy coverage (i.e. —the reappearance of green vegetation) rather than the ecological recovery of the pre-fire ecosystem. For forests in particular, the new vegetation that emerges after fire often differs significantly in species composition, structure, and ecological function from the original community (Durigan and Ratter, 2016; Maezumi et al., 2018; Mesquita et al., 2015).

# 5. Conclusions

The CAT region is a vital ecological zone in the tropics, characterized by frequent agricultural activities. Historically, there has been a significant gap in understanding the dynamics of vegetation disturbances in this area, at least in part due to the difficulty of detecting and identifying specific types of disturbance events across this spatially complex environment. This study provides the first regional-scale integration of LandTrendr temporal segmentation and deep learning-based classification (ResNet), offering a novel framework to investigate the spatiotemporal dynamics of vegetation disturbances in the CAT over the past 35 years. By distinguishing disturbance categories and evaluating their temporal trajectories, our analysis sheds light on the divergent responses of Amazon forest and Cerrado vegetation to disturbance events across the CAT. Our findings indicate that between 1986 and 2020, the CAT region experienced disturbances covering more than 384,000 km2. Amazon forest clear-cutting emerged as the most prevalent disturbance type (35%), but clear-cutting activities in the Cerrado vegetation accounted for almost a quarter (24%) of the detected disturbance events. Whilst Amazon forest disturbances tend to be more concentrated, often representing encroachments into the natural boundaries of the Amazon forest, the Cerrado vegetation is undergoing severe fragmentation often driven by agricultural activities, which result in long-term vegetation loss. In addition, fires, though less destructive in the short term, often prevent full recovery in the long term, particularly in the fire-adapted yet increasingly vulnerable Cerrado vegetation.

These findings offer valuable insights for future ecological conservation and management efforts in the CAT and underscore the critical importance of protecting these key transitional ecoregions in the context of global climate change. The combined use of interpretable temporal segmentation and high-capacity classification models provides a scalable and transferable methodology for large-area disturbance monitoring, enabling the identification of priority areas for conservation and intervention. By identifying areas with high disturbance frequencies and ecological vulnerabilities, we can more effectively formulate conservation strategies, optimize resource allocation, and enhance the resilience and adaptive capacity of ecosystems.

# **Author Contributions**

**Chuanze Li:** Writing – original draft, Writing – review & editing, Software, Visualization, Validation, Conceptualization, Methodology, Formal analysis, Data curation. **Angela Harris:** Writing – review &

editing, Supervision, Conceptualization, Methodology. **Beatriz Schwantes Marimon:** Writing – review & editing, Resources, Validation. **Ben Hur Marimon Junior:** Writing – review & editing, Resources, Validation. **Matthew Dennis:** Writing – review & editing, Supervision. **Ricardo Dalagnol:** Writing – review & editing. **Polyanna da Conceição Bispo:** Writing – review & editing, Supervision, Conceptualization, Methodology, Resources.

# **Funding**

This research did not receive any specific grant from funding agencies in the public, commercial, or not-for-profit sectors.

#### **Conflicts of Interest**

The authors declare no conflicts of interest.

#### References

Alencar, A., Asner, G.P., Knapp, D., Zarin, D., 2011. Temporal variability of forest fires in eastern Amazonia. Ecological Applications 21, 2397–2412. https://doi.org/10.1890/10-1168.1

Almeida, D., André, M., Scariot, E.C., Fushita, A.T., dos Santos, J.E., Bogaert, J., 2018. Temporal change of Distance to Nature index for anthropogenic influence monitoring in a protected area and its buffer zone. Ecological Indicators 91, 189–194. https://doi.org/10.1016/j.ecolind.2018.03.055

Almeida de Souza, A., Galvão, L.S., Korting, T.S., Prieto, J.D., 2020. Dynamics of savanna clearing and land degradation in the newest agricultural frontier in Brazil. GIScience & Remote Sensing 57, 965–984. https://doi.org/10.1080/15481603.2020.1835080

Alvarado, S.T., Fornazari, T., Cóstola, A., Morellato, L.P.C., Silva, T.S.F., 2017. Drivers of fire occurrence in a mountainous Brazilian cerrado savanna: Tracking long-term fire regimes using remote sensing. Ecological Indicators 78, 270–281. https://doi.org/10.1016/j.ecolind.2017.02.037

Andela, N., Morton, D.C., Giglio, L., Chen, Y., van der Werf, G.R., Kasibhatla, P.S., DeFries, R.S., Collatz, G.J., Hantson, S., Kloster, S., Bachelet, D., Forrest, M., Lasslop, G., Li, F., Mangeon, S., Melton, J.R., Yue, C., Randerson, J.T., 2017. A human-driven decline in global burned area. Science 356, 1356–1362. https://doi.org/10.1126/science.aal4108

Andreoni, M., Londoño, E., 2019. Amid outrage over Amazon forest fires, many in the Amazon remain defiant. [WWW Document]. The New York Times. URL

https://www.nytimes.com/2019/08/26/world/americas/brazil-amazon-rainforest-fire.html

Aragão, L.E.O.C., Anderson, L.O., Fonseca, M.G., Rosan, T.M., Vedovato, L.B., Wagner, F.H., Silva, C.V.J., Silva Junior, C.H.L., Arai, E., Aguiar, A.P., Barlow, J., Berenguer, E., Deeter, M.N., Domingues, L.G., Gatti, L., Gloor, M., Malhi, Y., Marengo, J.A., Miller, J.B., Phillips, O.L., Saatchi, S., 2018. 21st Century drought-related fires counteract the decline of Amazon deforestation carbon emissions. Nat Commun 9, 536. https://doi.org/10.1038/s41467-017-02771-y

Araújo, I., Marimon, B.S., Scalon, M.C., Fauset, S., Junior, B.H.M., Tiwari, R., Galbraith, D.R., Gloor, M.U., 2021. Trees at the Amazonia-Cerrado transition are approaching high temperature thresholds. Environ. Res. Lett. 16, 034047. https://doi.org/10.1088/1748-9326/abe3b9

Arroyo-Kalin, M., 2012. Slash-burn-and-churn: Landscape history and crop cultivation in pre-Columbian Amazonia. Quaternary International, Long-term perspectives on human occupation of tropical rainforests 249, 4–18. https://doi.org/10.1016/j.quaint.2011.08.004

Arvor, D., Tritsch, I., Barcellos, C., Jégou, N., Dubreuil, V., 2017. Land use sustainability on the South-Eastern Amazon agricultural frontier: Recent progress and the challenges ahead. Applied Geography 80, 86–97. https://doi.org/10.1016/j.apgeog.2017.02.003

Attri, V., Dhiman, R., Sarvade, S., 2020. A review on status, implications and recent trends of forest fire management. Arch. Agric. Environ. Sci. 5, 592–602. https://doi.org/10.26832/24566632.2020.0504024 Avery, T.E., Berlin, G.L., 1992. Fundamentals of remote sensing and airphoto interpretation, 5th ed. ed. Macmillan: Maxwell Macmillan International and Maxwell Macmillan Canada.

Bacha, C.J.C., Vinicios de Carvalho, L., 2014. What Explains the Intensification and Diversification of Brazil's Agricultural Production and Exports from 1990 to 2012? https://doi.org/10.2139/ssrn.2470995 Bai, M., Peng, P., Zhang, S., Wang, Xueman, Wang, Xiao, Wang, J., Pellikka, P., 2023. Mountain Forest Type Classification Based on One-Dimensional Convolutional Neural Network. Forests 14, 1823. https://doi.org/10.3390/f14091823

Balch, J.K., Nepstad, D.C., Curran, L.M., Brando, P.M., Portela, O., Guilherme, P., Reuning-Scherer, J.D., de Carvalho, O., 2011. Size, species, and fire behavior predict tree and liana mortality from experimental burns in the Brazilian Amazon. Forest Ecology and Management 261, 68–77. https://doi.org/10.1016/j.foreco.2010.09.029

Banskota, A., Kayastha, N., Falkowski, M.J., Wulder, M.A., Froese, R.E., White, J.C., 2014. Forest Monitoring Using Landsat Time Series Data: A Review. Canadian Journal of Remote Sensing 40, 362–384. https://doi.org/10.1080/07038992.2014.987376

Barreto, P. (Ed.), 2006. Human pressure on the Brazilian Amazon forests, WRI report. World Resources Institute, Washington, D.C.

Bendini, H.N., Fonseca, L.M.G., Matosak, B.M., Mariano, R.F., Haidar, R.F., Valeriano, D.M., 2022. Evaluating the separability between dry tropical forests and savanna woodlands in the Brazilian savanna using landsat dense image time series and artificial intelligence. The International Archives of the Photogrammetry, Remote Sensing and Spatial Information Sciences 43, 841–847.

https://doi.org/10.5194/isprs-archives-XLIII-B3-2022-841-2022

Bonini, I., Hur Marimon-Junior, B., Matricardi, E., Phillips, O., Petter, F., Oliveira, B., Marimon, B.S., 2018. Collapse of ecosystem carbon stocks due to forest conversion to soybean plantations at the Amazon-Cerrado transition. Forest Ecology and Management 414, 64–73.

https://doi.org/10.1016/j.foreco.2018.01.038

Bright, B.C., Hudak, A.T., Kennedy, R.E., Braaten, J.D., Henareh Khalyani, A., 2019. Examining post-fire vegetation recovery with Landsat time series analysis in three western North American forest types. fire ecol 15, 8. https://doi.org/10.1186/s42408-018-0021-9

Bullock, E.L., Woodcock, C.E., 2021. Carbon loss and removal due to forest disturbance and regeneration in the Amazon. Science of The Total Environment 764, 142839.

https://doi.org/10.1016/j.scitotenv.2020.142839

Carneiro, B.M., de Carvalho Junior, O.A., Guimarães, R.F., Evangelista, B.A., de Carvalho, O.L.F., 2024. Exploiting Legal Reserve Compensation as a Mechanism for Unlawful Deforestation in the Brazilian Cerrado Biome, 2012–2022. Sustainability 16, 9557. https://doi.org/10.3390/su16219557

Cerri, C.E.P., Cerri, C.C., Maia, S.M.F., Cherubin, M.R., Feigl, B.J., Lal, R., 2018. Reducing Amazon Deforestation through Agricultural Intensification in the Cerrado for Advancing Food Security and Mitigating Climate Change. Sustainability 10, 989. https://doi.org/10.3390/su10040989

Chen, Xi, Zhao, W., Chen, J., Qu, Y., Wu, D., Chen, Xuehong, 2021. Mapping Large-Scale Forest Disturbance Types with Multi-Temporal CNN Framework. Remote Sensing 13, 5177. https://doi.org/10.3390/rs13245177

Cochran, W.G., 1977. Sampling techniques. john wiley & sons.

Coe, M.T., Marthews, T.R., Costa, M.H., Galbraith, D.R., Greenglass, N.L., Imbuzeiro, H.M.A., Levine, N.M., Malhi, Y., Moorcroft, P.R., Muza, M.N., Powell, T.L., Saleska, S.R., Solorzano, L.A., Wang, J., 2013. Deforestation and climate feedbacks threaten the ecological integrity of south–southeastern Amazonia. Philosophical Transactions of the Royal Society B: Biological Sciences 368, 20120155. https://doi.org/10.1098/rstb.2012.0155

Cohen, W.B., Yang, Z., Kennedy, R., 2010. Detecting trends in forest disturbance and recovery using yearly Landsat time series: 2. TimeSync — Tools for calibration and validation. Remote Sensing of Environment 114, 2911–2924. https://doi.org/10.1016/j.rse.2010.07.010

Colman, C.B., Guerra, A., Almagro, A., de Oliveira Roque, F., Rosa, I.M., Fernandes, G.W., Oliveira, P.T.S., 2024. Modeling the Brazilian Cerrado land use change highlights the need to account for private property sizes for biodiversity conservation. Scientific Reports 14, 4559. https://doi.org/10.1038/s41598-024-55207-1

Connell, J.H., Slatyer, R.O., 1977. Mechanisms of Succession in Natural Communities and Their Role in Community Stability and Organization. The American Naturalist 111, 1119–1144. https://doi.org/10.1086/283241

Crist, E.P., Cicone, R.C., 1984. A physically-based transformation of Thematic Mapper data---The TM Tasseled Cap. IEEE Transactions on Geoscience and Remote sensing GE-22, 256–263. https://doi.org/10.1109/TGRS.1984.350619

da Silva Arruda, V.L., Alencar, A.A.C., de Carvalho Júnior, O.A., de Figueiredo Ribeiro, F., de Arruda, F.V., Conciani, D.E., da Silva, W.V., Shimbo, J.Z., 2024. Assessing four decades of fire behavior dynamics in the Cerrado biome (1985 to 2022). fire ecol 20, 1–20. https://doi.org/10.1186/s42408-024-00298-4

Dalagnol, R., Wagner, F.H., Galvão, L.S., Braga, D., Osborn, F., Sagang, L.B., da Conceição Bispo, P., Payne, M., Junior, C.S., Favrichon, S., 2023. Mapping tropical forest degradation with deep learning and Planet NICFI data. Remote Sensing of Environment 298, 113798.

https://doi.org/10.1016/j.rse.2023.113798

De Faria, B.L., Marano, G., Piponiot, C., Silva, C.A., Dantas, V. de L., Rattis, L., Rech, A.R., Collalti, A., 2021a. Model-Based Estimation of Amazonian Forests Recovery Time after Drought and Fire Events. Forests 12, 8. https://doi.org/10.3390/f12010008

De Faria, B.L., Staal, A., Silva, C.A., Martin, P.A., Panday, P.K., Dantas, V.L., 2021b. Climate change and deforestation increase the vulnerability of Amazonian forests to post-fire grass invasion. Global Ecology and Biogeography 30, 2368–2381. https://doi.org/10.1111/geb.13388

De Marco Jr, P., de Souza, R.A., FA Andrade, A., Villén-Pérez, S., Nóbrega, C.C., Campello, L.M., Caldas, M., 2023. The value of private properties for the conservation of biodiversity in the Brazilian Cerrado. Science 380, 298–301. https://doi.org/10.1126/science.abq7768

de Souza Mendes, F., Baron, D., Gerold, G., Liesenberg, V., Erasmi, S., 2019. Optical and SAR Remote Sensing Synergism for Mapping Vegetation Types in the Endangered Cerrado/Amazon Ecotone of Nova Mutum—Mato Grosso. Remote Sensing 11, 1161. https://doi.org/10.3390/rs11101161

DeVries, B., Decuyper, M., Verbesselt, J., Zeileis, A., Herold, M., Joseph, S., 2015. Tracking disturbance-regrowth dynamics in tropical forests using structural change detection and Landsat time series. Remote Sensing of Environment 169, 320–334. https://doi.org/10.1016/j.rse.2015.08.020 Dionizio, E.A., Costa, M.H., 2019. Influence of Land Use and Land Cover on Hydraulic and Physical Soil Properties at the Cerrado Agricultural Frontier. Agriculture 9, 24.

https://doi.org/10.3390/agriculture9010024

Dormann, C.F., Bagnara, M., Boch, S., Hinderling, J., Janeiro-Otero, A., Schäfer, D., Schall, P., Hartig, F., 2020. Plant species richness increases with light availability, but not variability, in temperate forests understorey. BMC Ecol 20, 1–9. https://doi.org/10.1186/s12898-020-00311-9

Drüke, M., Sakschewski, B., von Bloh, W., Billing, M., Lucht, W., Thonicke, K., 2023. Fire may prevent future Amazon forest recovery after large-scale deforestation. Commun Earth Environ 4, 248. https://doi.org/10.1038/s43247-023-00911-5

Durigan, G., Ratter, J.A., 2016. The need for a consistent fire policy for Cerrado conservation. Journal of Applied Ecology 53, 11–15. https://doi.org/10.1111/1365-2664.12559

Fang, X., Zhu, Q., Ren, L., Chen, H., Wang, K., Peng, C., 2018. Large-scale detection of vegetation dynamics and their potential drivers using MODIS images and BFAST: A case study in Quebec, Canada. Remote Sensing of Environment 206, 391–402. https://doi.org/10.1016/j.rse.2017.11.017

Faria, L.D. de, Matricardi, E.A.T., Marimon, B.S., Miguel, E.P., Junior, B.H.M., Oliveira, E.A. de,

Prestes, N.C.C. dos S., Carvalho, O.L.F. de, 2024. Biomass Prediction Using Sentinel-2 Imagery and an Artificial Neural Network in the Amazon/Cerrado Transition Region. Forests 15, 1599. https://doi.org/10.3390/f15091599

Fearnside, P.M., 2005. Deforestation in Brazilian Amazonia: History, Rates, and Consequences. Conservation Biology 19, 680–688. https://doi.org/10.1111/j.1523-1739.2005.00697.x

Ferreira de Alencar Mendes, B.T., Pinheiro, M.R., Barretto, E.H.P., Barreiros, A.M., Correia Furquim, S.A., Junqueira Villela, F.N., 2023. Impacts of Slash-and-Burn Cultivation on the Soil and Vegetation of the Atlantic Forest in Southeastern Brazil. Hum Ecol 51, 655–669. https://doi.org/10.1007/s10745-023-00429-6

Flores, B.M., Montoya, E., Sakschewski, B., Nascimento, N., Staal, A., Betts, R.A., Levis, C., Lapola, D.M., Esquível-Muelbert, A., Jakovac, C., 2024. Critical transitions in the Amazon forest system. Nature 626, 555–564. https://doi.org/10.1038/s41586-023-06970-0

Gao, B., 1996. NDWI—A normalized difference water index for remote sensing of vegetation liquid water from space. Remote Sensing of Environment 58, 257–266. https://doi.org/10.1016/S0034-4257(96)00067-3

Golin, T., 2024. The Southern Grasslands and the Expropriation of Indigenous Territories, in: Overbeck, G.E., Pillar, V.D.P., Müller, S.C., Bencke, G.A. (Eds.), South Brazilian Grasslands. Springer, Cham, pp. 145–174. https://doi.org/10.1007/978-3-031-42580-6 7

Gomes, L., Simões, S.J.C., Dalla Nora, E.L., de Sousa-Neto, E.R., Forti, M.C., Ometto, J.P.H.B., 2019. Agricultural Expansion in the Brazilian Cerrado: Increased Soil and Nutrient Losses and Decreased Agricultural Productivity. Land 8, 12. https://doi.org/10.3390/land8010012

Gómez, C., White, J.C., Wulder, M.A., 2011. Characterizing the state and processes of change in a dynamic forest environment using hierarchical spatio-temporal segmentation. Remote Sensing of Environment 115, 1665–1679. https://doi.org/10.1016/j.rse.2011.02.025

Gonçalves, R.V.S., Cardoso, J.C.F., Oliveira, P.E., Oliveira, D.C., 2021. Changes in the Cerrado vegetation structure: insights from more than three decades of ecological succession. Web Ecology 21, 55–64. https://doi.org/10.5194/we-21-55-2021

Gorelick, N., Hancher, M., Dixon, M., Ilyushchenko, S., Thau, D., Moore, R., 2017. Google Earth Engine: Planetary-scale geospatial analysis for everyone. Remote Sensing of Environment, Big Remotely Sensed Data: tools, applications and experiences 202, 18–27. https://doi.org/10.1016/j.rse.2017.06.031

Harding, T., Herzberg, J., Kuralbayeva, K., 2021. Commodity prices and robust environmental regulation: Evidence from deforestation in Brazil. Journal of Environmental Economics and Management 108, 102452. https://doi.org/10.1016/j.jeem.2021.102452

He, G., Shao, Z., Xing, S., Dong, D., Feng, X., 2016. Study on panchromatic and multispectral image fusion based on SFIM and CA transform, in: 2016 IEEE International Conference on Signal Processing, Communications and Computing (ICSPCC). IEEE, Hong Kong, China, pp. 1–6. https://doi.org/10.1109/ICSPCC.2016.7753705

Healey, S.P., Yang, Z., Cohen, W.B., Pierce, D.J., 2006. Application of two regression-based methods to estimate the effects of partial harvest on forest structure using Landsat data. Remote Sensing of Environment 101, 115–126. https://doi.org/10.1016/j.rse.2005.12.006

Hermosilla, T., Wulder, M.A., White, J.C., Coops, N.C., Hobart, G.W., 2015. Regional detection, characterization, and attribution of annual forest change from 1984 to 2012 using Landsat-derived timeseries metrics. Remote Sensing of Environment 170, 121–132. https://doi.org/10.1016/j.rse.2015.09.004 Hoffmann, W.A., 2005. Ecologia comparativa de espécies lenhosas de cerrado e de mata. Cerrado: Ecologia, Biodiversidade e Conservação. Brasília, DF: Ministério do Meio Ambiente 157–165.

Hoffmann, W.A., Geiger, E.L., Gotsch, S.G., Rossatto, D.R., Silva, L.C.R., Lau, O.L., Haridasan, M., Franco, A.C., 2012. Ecological thresholds at the savanna-forest boundary: how plant traits, resources and fire govern the distribution of tropical biomes. Ecology Letters 15, 759–768.

https://doi.org/10.1111/j.1461-0248.2012.01789.x

Huang, C., Goward, S.N., Schleeweis, K., Thomas, N., Masek, J.G., Zhu, Z., 2009. Dynamics of national forests assessed using the Landsat record: Case studies in eastern United States. Remote Sensing of

- Environment, Monitoring Protected Areas 113, 1430–1442. https://doi.org/10.1016/j.rse.2008.06.016 Hunke, P., Mueller, E.N., Schröder, B., Zeilhofer, P., 2015. The Brazilian Cerrado: assessment of water and soil degradation in catchments under intensive agricultural use. Ecohydrology 8, 1154–1180. https://doi.org/10.1002/eco.1573
- IBGE, 2019. Biomas e Sistema Costeiro-Marinho do Brasil.
- Kennedy, R.E., Yang, Z., Cohen, W.B., 2010. Detecting trends in forest disturbance and recovery using yearly Landsat time series: 1. LandTrendr Temporal segmentation algorithms. Remote Sensing of Environment 114, 2897–2910. https://doi.org/10.1016/j.rse.2010.07.008
- Kennedy, R.E., Yang, Z., Cohen, W.B., Pfaff, E., Braaten, J., Nelson, P., 2012. Spatial and temporal patterns of forest disturbance and regrowth within the area of the Northwest Forest Plan. Remote Sensing of Environment, Landsat Legacy Special Issue 122, 117–133. https://doi.org/10.1016/j.rse.2011.09.024 Kennedy, R.E., Yang, Z., Gorelick, N., Braaten, J., Cavalcante, L., Cohen, W.B., Healey, S., 2018. Implementation of the LandTrendr Algorithm on Google Earth Engine. Remote Sensing 10, 691. https://doi.org/10.3390/rs10050691
- Key, C.H., 2006. Ecological and Sampling Constraints on Defining Landscape Fire Severity. fire ecol 2, 34–59. https://doi.org/10.4996/fireecology.0202034
- Key, C.H., Benson, N.C., 2006. Landscape Assessment (LA). FIREMON: Fire effects monitoring and inventory system. Gen. Tech. Rep. RMRS-GTR-164-CD, Fort Collins, CO: US Department of Agriculture, Forest Service, Rocky Mountain Research Station. https://doi.org/10.2737/RMRS-GTR-164 Koonce, B., 2021. ResNet 50, in: Koonce, B. (Ed.), Convolutional Neural Networks with Swift for Tensorflow: Image Recognition and Dataset Categorization. Apress, Berkeley, CA, pp. 63–72. https://doi.org/10.1007/978-1-4842-6168-2 6
- Lenza, E., Santos, J.O., Maracahipes-Santos, L., 2015. Species composition, diversity, and vegetation structure in a gallery forest-*cerrado sensu stricto* transition zone in eastern Mato Grosso, Brazil. Acta Bot. Bras. 29, 327–338. https://doi.org/10.1590/0102-33062014abb3697
- Li, X., Jiang, H., Jiang, X., Shi, M., 2021. Identification of Geographical Origin of Chinese Chestnuts Using Hyperspectral Imaging with 1D-CNN Algorithm. Agriculture 11, 1274. https://doi.org/10.3390/agriculture11121274
- Li, Y., Xu, X., Wu, Z., Fan, H., Tong, X., Liu, J., 2022. A forest type-specific threshold method for improving forest disturbance and agent attribution mapping. GIScience & Remote Sensing 59, 1624–1642. https://doi.org/10.1080/15481603.2022.2127459
- Lucas, K.R.G., Caldarelli, C.E., Ventura, M.U., 2023. Agriculture and biodiversity damage: A prospective evaluation of the impact of Brazilian agriculture on its ecoregions through life cycle assessment methodology. Science of The Total Environment 899, 165762. https://doi.org/10.1016/j.scitotenv.2023.165762
- Luiz, C.H.P., Steinke, V.A., 2022. Recent Environmental Legislation in Brazil and the Impact on Cerrado Deforestation Rates. Sustainability 14, 8096. https://doi.org/10.3390/su14138096
- Ma, J., Zhang, C., Guo, H., Chen, W., Yun, W., Gao, L., Wang, H., 2020. Analyzing Ecological Vulnerability and Vegetation Phenology Response Using NDVI Time Series Data and the BFAST Algorithm. Remote Sensing 12, 3371. https://doi.org/10.3390/rs12203371
- Ma, Y., Zhen, Z., Li, F., Feng, F., Zhao, Y., 2023. An innovative lightweight 1D-CNN model for efficient monitoring of large-scale forest composition: a case study of Heilongjiang Province, China. GIScience & Remote Sensing 60, 2271246. https://doi.org/10.1080/15481603.2023.2271246
- Machida, W.S., Gomes, L., Moser, P., Castro, I.B., Miranda, S.C., da Silva-Júnior, M.C., Bustamante, M.M.C., 2021. Long term post-fire recovery of woody plants in savannas of central Brazil. Forest Ecology and Management 493, 119255. https://doi.org/10.1016/j.foreco.2021.119255
- Maezumi, S.Y., Robinson, M., de Souza, J., Urrego, D.H., Schaan, D., Alves, D., Iriarte, J., 2018. New Insights From Pre-Columbian Land Use and Fire Management in Amazonian Dark Earth Forests. Front. Ecol. Evol. 6. https://doi.org/10.3389/fevo.2018.00111
- Maia, S.M.F., Ogle, S.M., Cerri, C.E.P., Cerri, C.C., 2010. Soil organic carbon stock change due to land use activity along the agricultural frontier of the southwestern Amazon, Brazil, between 1970 and 2002.

Global Change Biology 16, 2775–2788. https://doi.org/10.1111/j.1365-2486.2009.02105.x Maracahipes, L., Marimon, B., Lenza, E., Marimon-Junior, B.H., Almeida de Oliveira, E., Mews, H., Gomes, L., Feldpausch, T., 2014. Post-fire dynamics of woody vegetation in seasonally flooded forests (impucas) in the Cerrado-Amazonian Forest transition zone. Flora - Morphology, Distribution, Functional Ecology of Plants 209. https://doi.org/10.1016/j.flora.2014.02.008

Maracahipes-Santos, L., Lenza, E., dos Santos, J.O., Marimon, B.S., Eisenlohr, P.V., Marimon Junior, B.H., Feldpausch, T.R., 2015. Diversity, floristic composition, and structure of the woody vegetation of the Cerrado in the Cerrado–Amazon transition zone in Mato Grosso, Brazil. Braz. J. Bot 38, 877–887. https://doi.org/10.1007/s40415-015-0186-2

Maretto, R.V., Fonseca, L.M., Jacobs, N., Körting, T.S., Bendini, H.N., Parente, L.L., 2020. Spatiotemporal deep learning approach to map deforestation in amazon rainforest. IEEE Geoscience and Remote Sensing Letters 18, 771–775. https://doi.org/10.1109/LGRS.2020.2986407

Marimon, B.S., Lima, E.D.S., Duarte, T.G., Chieregatto, L.C., Ratter, J.A., 2006. OBSERVATIONS ON THE VEGETATION OF NORTHEASTERN MATO GROSSO, BRAZIL. IV. AN ANALYSIS OF THE CERRADO–AMAZONIAN FOREST ECOTONE. Edinburgh Journal of Botany 63, 323–341. https://doi.org/10.1017/S0960428606000576

Marimon, B.S., Marimon-Junior, B.H., Feldpausch, T.R., Oliveira-Santos, C., Mews, H.A., Lopez-Gonzalez, G., Lloyd, J., Franczak, D.D., de Oliveira, E.A., Maracahipes, L., Miguel, A., Lenza, E., Phillips, O.L., 2014. Disequilibrium and hyperdynamic tree turnover at the forest–cerrado transition zone in southern Amazonia. Plant Ecology & Diversity 7, 281–292. https://doi.org/10.1080/17550874.2013.818072

Marimon Junior, B.H., Haridasan, M., 2005. Comparação da vegetação arbórea e características edáficas de um cerradão e um cerrado sensu stricto em áreas adjacentes sobre solo distrófico no leste de Mato Grosso, Brasil. Acta botânica brasílica 19, 913–926.

Marques, E.Q., Marimon-Junior, B.H., Marimon, B.S., Matricardi, E.A.T., Mews, H.A., Colli, G.R., 2020. Redefining the Cerrado–Amazonia transition: implications for conservation. Biodivers Conserv 29, 1501–1517. https://doi.org/10.1007/s10531-019-01720-z

Marques, E.Q., Silvério, D.V., Galvão, L.S., Aragão, L.E.O.C., Uribe, M.R., Macedo, M.N., Rattis, L., Alencar, A.A.C., Brando, P.M., 2024. Assessing the effectiveness of vegetation indices in detecting forest disturbances in the southeast Amazon. Sci Rep 14, 27287. https://doi.org/10.1038/s41598-024-77924-3 Martello, F., dos Santos, J.S., Silva-Neto, C.M., Cássia-Silva, C., Siqueira, K.N., Ataíde, M.V.R. de, Ribeiro, M.C., Collevatti, R.G., 2023. Landscape structure shapes the diversity of plant reproductive traits in agricultural landscapes in the Brazilian Cerrado. Agriculture, Ecosystems & Environment 341, 108216. https://doi.org/10.1016/j.agee.2022.108216

Matricardi, E.A.T., Skole, D.L., Costa, O.B., Pedlowski, M.A., Samek, J.H., Miguel, E.P., 2020. Long-term forest degradation surpasses deforestation in the Brazilian Amazon. Science 369, 1378–1382. https://doi.org/10.1126/science.abb3021

Matricardi, E.A.T., Skole, D.L., Pedlowski, M.A., Chomentowski, W., 2013. Assessment of forest disturbances by selective logging and forest fires in the Brazilian Amazon using Landsat data. International Journal of Remote Sensing 34, 1057–1086. https://doi.org/10.1080/01431161.2012.717182 Medeiros, M.B. de, Fiedler, N.C., 2011. Heterogeneidade de ecossistemas, modelos de desequilíbrio e distúrbios. Biodiversidade Brasileira 1, 4–11. https://doi.org/10.37002/biodiversidadebrasileira.v1i2.135 Melo, P., Sparacino, J., Argibay, D., Sousa Júnior, V., Barros, R., Espindola, G., 2021. Assessing Wildfire Regimes in Indigenous Lands of the Brazilian Savannah-Like Cerrado. Fire 4, 34. https://doi.org/10.3390/fire4030034

Mesquita, R.C.G., Massoca, P.E. dos S., Jakovac, C.C., Bentos, T.V., Williamson, G.B., 2015. Amazon Rain Forest Succession: Stochasticity or Land-Use Legacy? BioScience 65, 849–861. https://doi.org/10.1093/biosci/biv108

Miller, J.D., Knapp, E.E., Key, C.H., Skinner, C.N., Isbell, C.J., Creasy, R.M., Sherlock, J.W., 2009. Calibration and validation of the relative differenced Normalized Burn Ratio (RdNBR) to three measures of fire severity in the Sierra Nevada and Klamath Mountains, California, USA. Remote Sensing of

Environment 113, 645–656. https://doi.org/10.1016/j.rse.2008.11.009

Miller, J.D., Thode, A.E., 2007. Quantifying burn severity in a heterogeneous landscape with a relative version of the delta Normalized Burn Ratio (dNBR). Remote Sensing of Environment 109, 66–80. https://doi.org/10.1016/j.rse.2006.12.006

Miranda, H.S., Sato, M.N., Neto, W.N., Aires, F.S., 2009. Fires in the cerrado, the Brazilian savanna, in: Cochrane, M.A. (Ed.), Tropical Fire Ecology: Climate Change, Land Use, and Ecosystem Dynamics. Springer, Berlin, Heidelberg, pp. 427–450. https://doi.org/10.1007/978-3-540-77381-8 15

Moreira, A.G., 2000. Effects of fire protection on savanna structure in Central Brazil. Journal of Biogeography 27, 1021–1029. https://doi.org/10.1046/j.1365-2699.2000.00422.x

Morton, D.C., DeFries, R.S., Shimabukuro, Y.E., Anderson, L.O., Arai, E., del Bon Espirito-Santo, F., Freitas, R., Morisette, J., 2006. Cropland expansion changes deforestation dynamics in the southern Brazilian Amazon. Proceedings of the National Academy of Sciences 103, 14637–14641. https://doi.org/10.1073/pnas.0606377103

Mota, F.B. da S., Ferreira, K.R., Escada, M.I.S., 2024. Evaluating Forest Disturbance Detection Methods based on Satellite Image Time Series for Amazon Deforestation Alerts. The International Archives of the Photogrammetry, Remote Sensing and Spatial Information Sciences XLVIII-3–2024, 357–364. https://doi.org/10.5194/isprs-archives-XLVIII-3-2024-357-2024

Murillo-Sandoval, P.J., Hilker, T., Krawchuk, M.A., Van Den Hoek, J., 2018. Detecting and Attributing Drivers of Forest Disturbance in the Colombian Andes Using Landsat Time-Series. Forests 9, 269. https://doi.org/10.3390/f9050269

Myers, N., 2023. Tropical deforestation: rates and patterns. The causes of tropical deforestation 27–40. Nepstad, D.C., Stickler, C.M., Almeida, O.T., 2006. Globalization of the Amazon Soy and Beef Industries: Opportunities for Conservation. Conservation Biology 20, 1595–1603. https://doi.org/10.1111/j.1523-1739.2006.00510.x

Novo-Fernández, A., Franks, S., Wehenkel, C., López-Serrano, P.M., Molinier, M., López-Sánchez, C.A., 2018. Landsat time series analysis for temperate forest cover change detection in the Sierra Madre Occidental, Durango, Mexico. International Journal of Applied Earth Observation and Geoinformation 73, 230–244. https://doi.org/10.1016/j.jag.2018.06.015

Ochtyra, A., 2020. Forest Disturbances in Polish Tatra Mountains for 1985–2016 in Relation to Topography, Stand Features, and Protection Zone. Forests 11, 579. https://doi.org/10.3390/f11050579 Oliveira, B. de, Junior, B.H.M., Mews, H.A., Valadao, M.B.X., Marimon, B.S., 2017. Unraveling the ecosystem functions in the Amazonia-Cerrado transition: evidence of hyperdynamic nutrient cycling. Plant Ecology 218, 225–240. https://doi.org/10.1007/s11258-016-0681-y

Ouma, S., 2020. Farming as Financial Asset: Global Finance and the Making of Institutional Landscapes. Agenda Publishing Limited.

Pellegrini, A.F.A., Ahlström, A., Hobbie, S.E., Reich, P.B., Nieradzik, L.P., Staver, A.C., Scharenbroch, B.C., Jumpponen, A., Anderegg, W.R.L., Randerson, J.T., Jackson, R.B., 2018. Fire frequency drives decadal changes in soil carbon and nitrogen and ecosystem productivity. Nature 553, 194–198. https://doi.org/10.1038/nature24668

Perbet, P., Guindon, L., Côté, J.-F., Béland, M., 2024. Evaluating deep learning methods applied to Landsat time series subsequences to detect and classify boreal forest disturbances events: The challenge of partial and progressive disturbances. Remote Sensing of Environment 306, 114107.

Pfeiffer, J., Ruder, S., Vulić, I., Ponti, E.M., 2023. Modular deep learning. arXiv preprint arXiv:2302.11529. https://doi.org/10.48550/arXiv.2302.11529

Pinty, B., Verstraete, M.M., Gobron, N., Roveda, F., Govaerts, Y., 2000. Do man-made fires affect Earth's surface reflectance at continental scales? Eos, Transactions American Geophysical Union 81, 381–389. https://doi.org/10.1029/00EO00281

Pivello, V.R., Vieira, I., Christianini, A.V., Ribeiro, D.B., da Silva Menezes, L., Berlinck, C.N., Melo, F.P.L., Marengo, J.A., Tornquist, C.G., Tomas, W.M., Overbeck, G.E., 2021. Understanding Brazil's catastrophic fires: Causes, consequences and policy needed to prevent future tragedies. Perspectives in Ecology and Conservation 19, 233–255. https://doi.org/10.1016/j.pecon.2021.06.005

- Pokorny, B., Pacheco, P., 2014. Money from and for forests: A critical reflection on the feasibility of market approaches for the conservation of Amazonian forests. Journal of Rural Studies 36, 441–452. https://doi.org/10.1016/j.jrurstud.2014.09.004
- Pokorny, B., Pacheco, P., de Jong, W., Entenmann, S.K., 2021. Forest frontiers out of control: The long-term effects of discourses, policies, and markets on conservation and development of the Brazilian Amazon. Ambio 50, 2199–2223. https://doi.org/10.1007/s13280-021-01637-4
- Pokorny, B., Scholz, I., De Jong, W., 2013. REDD+ for the poor or the poor for REDD+? About the limitations of environmental policies in the Amazon and the potential of achieving environmental goals through pro-poor policies. Ecology and Society 18. https://www.jstor.org/stable/26269329
- Projeto RADAMBRASIL, 1981., in: Folha SD.22 Goiás: Geologia, Geomorfologia, Pedologia, Vegetação, Uso Potencial Da Terra, Levantamento de Recursos Naturais. Ministério das Minas e Energia. Secretaria Geral, Rio de Janeiro, p. 636.
- Ratter, J.A., Richards, P.W., Argent, G., Gifford, D.R., Clapham, A.R., 1973. Observations on the vegetation of northeastern Mato Grosso: I. The woody vegetation types of the Xavantina-Cachimbo Expedition Area. Philosophical Transactions of the Royal Society of London. B, Biological Sciences 266, 449–492. https://doi.org/10.1098/rstb.1973.0053
- Reis, S.M., de Oliveira, E.A., Elias, F., Gomes, L., Morandi, P.S., Marimon, B.S., Marimon Junior, B.H., das Neves, E.C., de Oliveira, B., Lenza, E., 2017. Resistance to fire and the resilience of the woody vegetation of the "Cerradão" in the "Cerrado"–Amazon transition zone. Braz. J. Bot 40, 193–201. https://doi.org/10.1007/s40415-016-0336-1
- Reis, S.M., Lenza, E., Marimon, B.S., Gomes, L., Forsthofer, M., Morandi, P.S., Marimon Junior, B.H., Feldpausch, T.R., Elias, F., 2015. Post-fire dynamics of the woody vegetation of a savanna forest (Cerradão) in the Cerrado-Amazon transition zone. Acta Bot. Bras. 29, 408–416. https://doi.org/10.1590/0102-33062015abb0009
- Reis, S.M., Marimon, B.S., Marimon Junior, B.H., Morandi, P.S., Oliveira, E.A. de, Elias, F., Neves, E.C. das, Oliveira, B. de, Nogueira, D. da S., Umetsu, R.K., Feldpausch, T.R., Phillips, O.L., 2018. Climate and fragmentation affect forest structure at the southern border of Amazonia. Plant Ecology & Diversity 11, 13–25. https://doi.org/10.1080/17550874.2018.1455230
- Reygadas, Y., Spera, S., Galati, V., Salisbury, D.S., Silva, S., Novoa, S., 2021. Mapping forest disturbances across the Southwestern Amazon: tradeoffs between open-source, Landsat-based algorithms. Environ. Res. Commun. 3, 091001. https://doi.org/10.1088/2515-7620/ac2210
- Ribeiro, A.F.S., Santos, L., Randerson, J.T., Uribe, M.R., Alencar, A.A.C., Macedo, M.N., Morton, D.C., Zscheischler, J., Silvestrini, R.A., Rattis, L., Seneviratne, S.I., Brando, P.M., 2024. The time since landuse transition drives changes in fire activity in the Amazon-Cerrado region. Commun Earth Environ 5, 96. https://doi.org/10.1038/s43247-024-01248-3
- Ribeiro, J.F., Walter, B.M.T., 2008. As principais fitofissionomias do bioma cerrado., in: Cerrado: Ecologia e Flora. pp. 151–212.
- Ribeiro, J.M.P., Maculan, G., de Ávila, B.O., Morais, V.A., Hoeckesfeld, L., Secchi, L., de Andrade Guerra, J.B.S.O., 2025. Deforestation by production displacement: expansion of cropland and cattle ranching on Amazon Forest. Environment, Development and Sustainability 1–32. https://doi.org/10.1007/s10668-024-05917-3
- Rodrigues, C.A., Zirondi, H.L., Fidelis, A., 2021. Fire frequency affects fire behavior in open savannas of the Cerrado. Forest Ecology and Management 482, 118850. https://doi.org/10.1016/j.foreco.2020.118850 Rosan, T.M., Sitch, S., Mercado, L.M., Heinrich, V., Friedlingstein, P., Aragão, L.E.O.C., 2022.
- Fragmentation-Driven Divergent Trends in Burned Area in Amazonia and Cerrado. Frontiers in Forests and Global Change 5. https://doi.org/10.3389/ffgc.2022.801408
- Ros-Tonen, M.A., Van Andel, T., Morsello, C., Otsuki, K., Rosendo, S., Scholz, I., 2008. Forest-related partnerships in Brazilian Amazonia: there is more to sustainable forest management than reduced impact logging. Forest Ecology and Management 256, 1482–1497. https://doi.org/10.1016/j.foreco.2008.02.044 Roy, D.P., Kovalskyy, V., Zhang, H.K., Vermote, E.F., Yan, L., Kumar, S.S., Egorov, A., 2016. Characterization of Landsat-7 to Landsat-8 reflective wavelength and normalized difference vegetation

index continuity. Remote Sensing of Environment, Landsat 8 Science Results 185, 57–70. https://doi.org/10.1016/j.rse.2015.12.024

Salimans, T., Kingma, D.P., 2016. Weight normalization: A simple reparameterization to accelerate training of deep neural networks. Advances in neural information processing systems 29.

Sano, E.E., 2019. Land Use Expansion in the Brazilian Cerrado, in: Hosono, A., Hamaguchi, N., Bojanic, A. (Eds.), Innovation with Spatial Impact: Sustainable Development of the Brazilian Cerrado. Springer, Singapore, pp. 137–162. https://doi.org/10.1007/978-981-13-6182-1 5

Santana, N.C., Júnior, O.A. de C., Gomes, R.A.T., Fontes Guimarães, R., 2020. Comparison of Post-fire Patterns in Brazilian Savanna and Tropical Forest from Remote Sensing Time Series. ISPRS International Journal of Geo-Information 9, 659. https://doi.org/10.3390/ijgi9110659

Sawyer, D., 2008. Climate change, biofuels and eco-social impacts in the Brazilian Amazon and Cerrado. Philosophical Transactions of the Royal Society B: Biological Sciences 363, 1747–1752. https://doi.org/10.1098/rstb.2007.0030

Schmidt, M.V.C., Ikpeng, Y.U., Kayabi, T., Sanches, R.A., Ono, K.Y., Adams, C., 2021. Indigenous Knowledge and Forest Succession Management in the Brazilian Amazon: Contributions to Reforestation of Degraded Areas. Front. For. Glob. Change 4. https://doi.org/10.3389/ffgc.2021.605925

Schroeder, T.A., Wulder, M.A., Healey, S.P., Moisen, G.G., 2011. Mapping wildfire and clearcut harvest disturbances in boreal forests with Landsat time series data. Remote Sensing of Environment 115, 1421–1433. https://doi.org/10.1016/j.rse.2011.01.022

Shimizu, K., Ota, T., Mizoue, N., Yoshida, S., 2019. A comprehensive evaluation of disturbance agent classification approaches: Strengths of ensemble classification, multiple indices, spatio-temporal variables, and direct prediction. ISPRS Journal of Photogrammetry and Remote Sensing 158, 99–112. https://doi.org/10.1016/j.isprsjprs.2019.10.004

Silva, C.V.J., Aragão, L.E.O.C., Barlow, J., Espirito-Santo, F., Young, P.J., Anderson, L.O., Berenguer, E., Brasil, I., Foster Brown, I., Castro, B., Farias, R., Ferreira, J., França, F., Graça, P.M.L.A., Kirsten, L., Lopes, A.P., Salimon, C., Scaranello, M.A., Seixas, M., Souza, F.C., Xaud, H.A.M., 2018. Drought-induced Amazonian wildfires instigate a decadal-scale disruption of forest carbon dynamics. Philosophical Transactions of the Royal Society B: Biological Sciences 373, 20180043. https://doi.org/10.1098/rstb.2018.0043

Silva Junior, C.H.L., Aragão, L.E.O.C., Anderson, L.O., Fonseca, M.G., Shimabukuro, Y.E., Vancutsem, C., Achard, F., Beuchle, R., Numata, I., Silva, C.A., Maeda, E.E., Longo, M., Saatchi, S.S., 2020. Persistent collapse of biomass in Amazonian forest edges following deforestation leads to unaccounted carbon losses. Science Advances 6, eaaz8360. https://doi.org/10.1126/sciadv.aaz8360

Souza, A.A. de, Galvão, L.S., Korting, T.S., Almeida, C.A., 2021. On a Data-Driven Approach for Detecting Disturbance in the Brazilian Savannas Using Time Series of Vegetation Indices. Remote Sensing 13, 4959. https://doi.org/10.3390/rs13244959

Souza-Alonso, P., Saiz, G., García, R.A., Pauchard, A., Ferreira, A., Merino, A., 2022. Post-fire ecological restoration in Latin American forest ecosystems: Insights and lessons from the last two decades. Forest Ecology and Management 509, 120083. https://doi.org/10.1016/j.foreco.2022.120083 Torello-Raventos, M., Feldpausch, T.R., Veenendaal, E., Schrodt, F., Saiz, G., Domingues, T.F., Djagbletey, G., Ford, A., Kemp, J., Marimon, B.S., Hur Marimon Junior, B., Lenza, E., Ratter, J.A., Maracahipes, L., Sasaki, D., Sonké, B., Zapfack, L., Taedoumg, H., Villarroel, D., Schwarz, M., Quesada, C.A., Yoko Ishida, F., Nardoto, G.B., Affum-Baffoe, K., Arroyo, L., M.J.S. Bowman, D., Compaore, H., Davies, K., Diallo, A., Fyllas, N.M., Gilpin, M., Hien, F., Johnson, M., Killeen, T.J., Metcalfe, D., Miranda, H.S., Steininger, M., Thomson, J., Sykora, K., Mougin, E., Hiernaux, P., Bird, M.I., Grace, J., Lewis, S.L., Phillips, O.L., Lloyd, J., 2013. On the delineation of tropical vegetation types with an emphasis on forest/savanna transitions. Plant Ecology & Diversity 6, 101–137. https://doi.org/10.1080/17550874.2012.762812

Vancutsem, C., Achard, F., Pekel, J.-F., Vieilledent, G., Carboni, S., Simonetti, D., Gallego, J., Aragão, L.E.O.C., Nasi, R., 2021. Long-term (1990–2019) monitoring of forest cover changes in the humid tropics. Science Advances 7, eabe1603. https://doi.org/10.1126/sciadv.abe1603

Verbesselt, J., Hyndman, R., Newnham, G., Culvenor, D., 2010. Detecting trend and seasonal changes in satellite image time series. Remote Sensing of Environment 114, 106–115. https://doi.org/10.1016/j.rse.2009.08.014

Verburg, R., Rodrigues Filho, S., Lindoso, D., Debortoli, N., Litre, G., Bursztyn, M., 2014. The impact of commodity price and conservation policy scenarios on deforestation and agricultural land use in a frontier area within the Amazon. Land use policy 37, 14–26. https://doi.org/10.1016/j.landusepol.2012.10.003 Vieira, L.T.A., Azevedo, T.N., Castro, A.A.J.F., Martins, F.R., 2022. Reviewing the Cerrado's limits, flora distribution patterns, and conservation status for policy decisions. Land Use Policy 115, 106038. https://doi.org/10.1016/j.landusepol.2022.106038

Wang, Y., Ziv, G., Adami, M., Mitchard, E., Batterman, S.A., Buermann, W., Schwantes Marimon, B., Marimon Junior, B.H., Matias Reis, S., Rodrigues, D., Galbraith, D., 2019. Mapping tropical disturbed forests using multi-decadal 30 m optical satellite imagery. Remote Sensing of Environment 221, 474–488. https://doi.org/10.1016/j.rse.2018.11.028

Wearn, O.R., Reuman, D.C., Ewers, R.M., 2012. Extinction Debt and Windows of Conservation Opportunity in the Brazilian Amazon. Science 337, 228–232. https://doi.org/10.1126/science.1219013 Wei-Jian, H., Yong-Tao, L., Yuan, H., 2021. Prediction of chaotic time series using hybrid neural network and attention mechanism. Acta Physica Sinica 70.

Yin, F., Lewis, P.E., Gómez-Dans, J.L., 2022. Bayesian atmospheric correction over land: Sentinel-2/MSI and Landsat 8/OLI. Geoscientific Model Development 15, 7933–7976. https://doi.org/10.5194/gmd-15-7933-2022

Zaiatz, A.P.S.R., Zolin, C.A., Vendrusculo, L.G., Lopes, T.R., Paulino, J., 2018. Agricultural land use and cover change in the Cerrado/Amazon ecotone: A case study of the upper Teles Pires River basin. Acta Amaz. 48, 168–177. https://doi.org/10.1590/1809-4392201701930

Zhao, F., Huang, C., Zhu, Z., 2015. Use of Vegetation Change Tracker and Support Vector Machine to Map Disturbance Types in Greater Yellowstone Ecosystems in a 1984–2010 Landsat Time Series. IEEE Geoscience and Remote Sensing Letters 12, 1650–1654. https://doi.org/10.1109/LGRS.2015.2418159 Zhou, M., Han, X., Wang, J., Ji, X., Zhou, Y., Liu, M., 2024. Identification and Mapping of Eucalyptus Plantations in Remote Sensing Data Using CCDC Algorithm and Random Forest. Forests 15, 1866. https://doi.org/10.3390/f15111866

Zhu, Z., Woodcock, C.E., 2014. Continuous change detection and classification of land cover using all available Landsat data. Remote Sensing of Environment 144, 152–171. https://doi.org/10.1016/j.rse.2014.01.011

Zhu, Z., Woodcock, C.E., 2012. Object-based cloud and cloud shadow detection in Landsat imagery. Remote Sensing of Environment 118, 83–94. https://doi.org/10.1016/j.rse.2011.10.028